

# Quantum Molecular Dynamics Simulations

---

Aiichiro Nakano

*Collaboratory for Advanced Computing & Simulations*

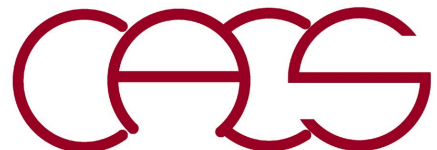
*Department of Computer Science*

*Department of Physics & Astronomy*

*Department of Quantitative & Computational Biology*

*University of Southern California*

Email: [anakano@usc.edu](mailto:anakano@usc.edu)

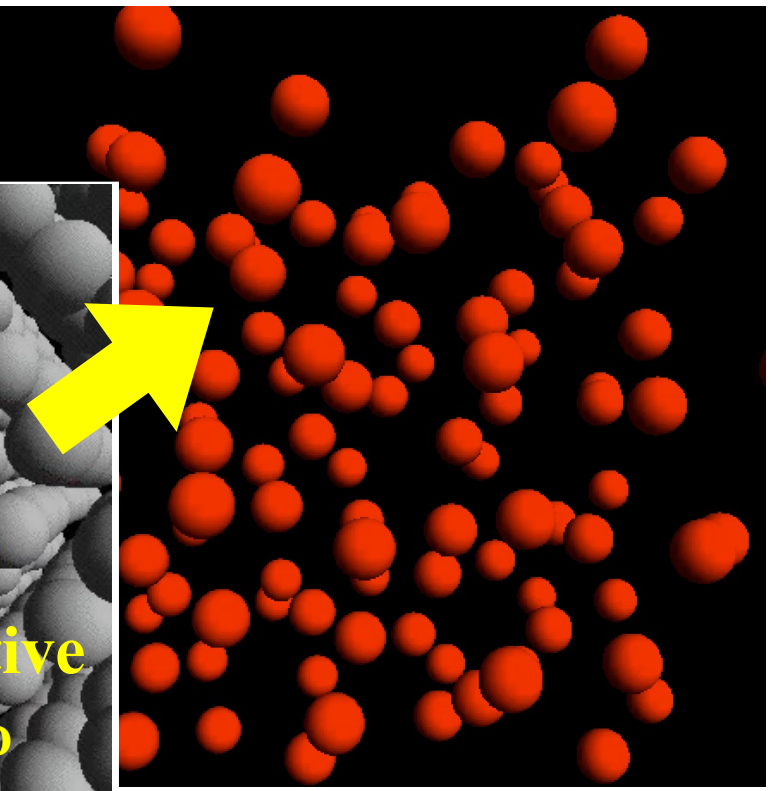
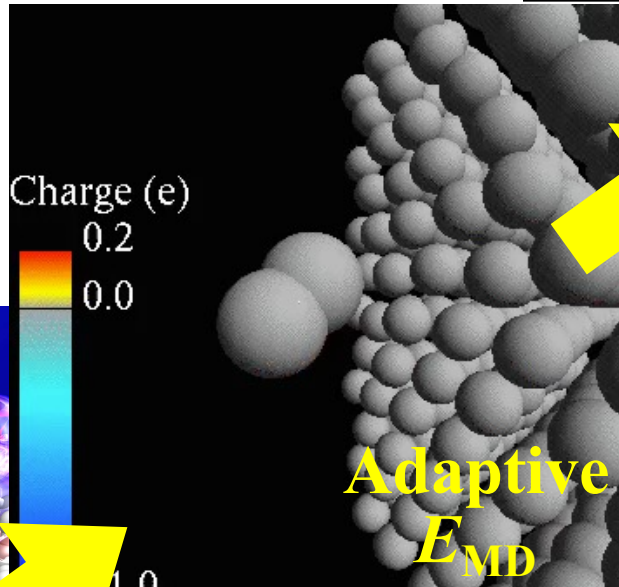


# Molecular Dynamics Hierarchy

## Molecular Dynamics (MD)

### Reactive MD (RMD)

### Nonadiabatic quantum MD (NAQMD)



### First principles-based reactive force-fields

- Reactive bond order  $\{BO_{ij}\}$   
→ Bond breakage & formation
- Charge equilibration (QEeq)  $\{q_i\}$   
→ Charge transfer

# Quantum Molecular Dynamics (QMD)

$$M_I \frac{d^2}{dt^2} \mathbf{R}_I = -\frac{\partial}{\partial \mathbf{R}_I} E[\{\mathbf{R}_I\}, \psi(\mathbf{r}_1, \dots, \mathbf{r}_N)] \quad (I = 1, \dots, N_{\text{atom}})$$

**First molecular dynamics using an empirical interatomic interaction**

A. Rahman, *Phys. Rev.* **136**, A405 ('64)

$$\psi(\mathbf{r}_1, \dots, \mathbf{r}_N) \leftarrow \operatorname{argmin} E[\{\mathbf{R}_I\}, \psi(\mathbf{r}_1, \dots, \mathbf{r}_N)]$$

**Density functional theory (DFT)**

Hohenberg & Kohn, *Phys. Rev.* **136**, B864 ('64)

W. Kohn, *Nobel chemistry prize*, '98

$O(C^N)$   $\rightarrow$   $O(N^3)$   
1  $N$ -electron problem  $\rightarrow$   $N$  1-electron problems  
intractable  $\rightarrow$  tractable

$$\psi(\mathbf{r}_1, \dots, \mathbf{r}_N) \quad \{\psi_i(\mathbf{r}) | i = 1, \dots, N\}$$

## $O(N)$ DFT algorithms

- **Divide-&-conquer DFT** [W. Yang, *Phys. Rev. Lett.* **66**, 1438 ('91); F. Shimojo *et al.*, *Comput. Phys. Commun.* **167**, 151 ('05); *Phys. Rev. B* **77**, 085103 ('08); *Appl. Phys. Lett.* **95**, 043114 ('09); *J. Chem. Phys.* **140**, 18A529 ('14)]
- **Quantum nearsightedness principle** [W. Kohn, *Phys. Rev. Lett.* **76**, 3168 ('96)]
- **A recent review** [Bowler & Miyazaki, *Rep. Prog. Phys.* **75**, 036503 ('12)]

# Born-Oppenheimer Approximation

- Consider a system of  $N$  electrons &  $N_{\text{atom}}$  nuclei, with the Hamiltonian

$$\begin{aligned}\tilde{H} &= \sum_{I=1}^{N_{\text{atom}}} \frac{\mathbf{P}_I^2}{2M_I} + H(\{\mathbf{r}_i\}, \{\mathbf{R}_I\}) \\ &= \sum_{I=1}^{N_{\text{atom}}} \left[ \frac{\mathbf{P}_I^2}{2M_I} + V_{\text{ext}}(\mathbf{R}_I) \right] + \sum_{i=1}^N \left[ -\frac{\hbar^2}{2m} \frac{\partial^2}{\partial \mathbf{r}_i^2} + v_{\text{ext}}(\mathbf{r}_i) \right] \\ &\quad + \frac{1}{2} \sum_{i \neq j} \frac{e^2}{|\mathbf{r}_i - \mathbf{r}_j|} - \sum_{i,J} \frac{Z_J e^2}{|\mathbf{r}_i - \mathbf{R}_J|} + \frac{1}{2} \sum_{I \neq J} \frac{Z_I Z_J e^2}{|\mathbf{R}_I - \mathbf{R}_J|}\end{aligned}$$

nucleus momentum  
electron position      nucleus position

nucleus charge

- Due to the much larger nuclei masses ( $M_I$ ) compared to the electron mass ( $m$ ), the quantum-mechanical wave function of the system is separable to those of the electrons & nuclei
- At ambient conditions, the electronic wave function remains in its ground state ( $|\Psi_0\rangle$ ) corresponding to the instantaneous nuclei positions ( $\{\mathbf{R}_I\}$ ), with the latter following classical mechanics

$$M_I \frac{d^2}{dt^2} \mathbf{R}_I = -\frac{\partial}{\partial \mathbf{R}_I} \langle \Psi_0 | H(\{\mathbf{r}_i\}, \{\mathbf{R}_I\}) | \Psi_0 \rangle$$

# Complexity Reduction: Density Functional Theory

- P. Hohenberg & W. Kohn, “Inhomogeneous electron gas”

*Phys. Rev.* **136**, B864 ('64)

The electronic ground state is a functional of the electron density  $\rho(\mathbf{r})$

- W. Kohn & L. Sham, “Self-consistent equations including exchange & correlation effects” *Phys. Rev.* **140**, A1133 ('65)

Derived a formally exact self-consistent single-electron equations for a many-electron system



# Kohn-Sham Energy Eigenstates

- Time-independent Schrödinger equation

$$\begin{array}{ccc} \text{Hamiltonian} & \longrightarrow & H\psi_n(\mathbf{r}) = \epsilon_n \psi_n(\mathbf{r}) \\ \text{operator} & & \longleftarrow \text{Eigenstate} \\ & & \text{Eigenvalue} \end{array}$$

- Stationary state

$$i\hbar \frac{\partial}{\partial t} \psi(t) = H\psi(t)$$

$$\psi(t) = \exp(-i\epsilon_n t/\hbar) \psi_n$$

- Hamiltonian operator

$$H = -\frac{\hbar^2}{2m} \frac{\partial^2}{\partial \mathbf{r}_i^2} + v(\mathbf{r})$$

- Density functional theory\*

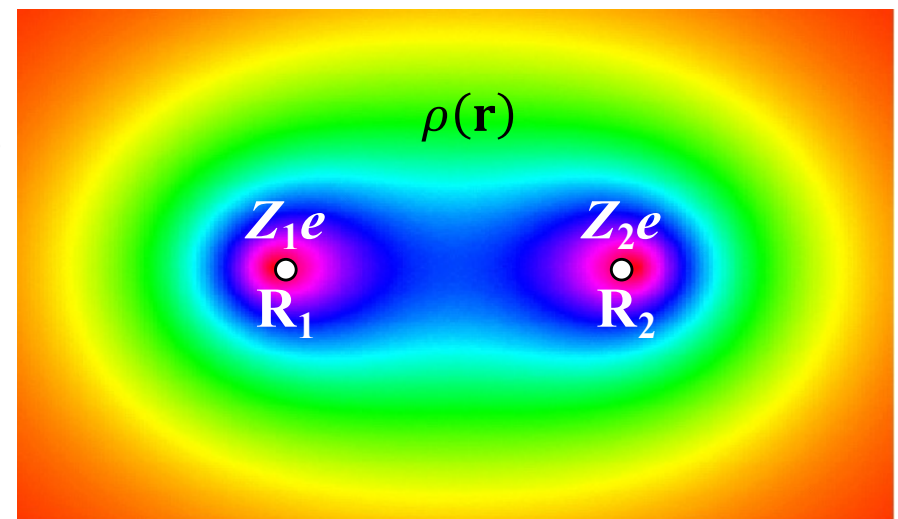
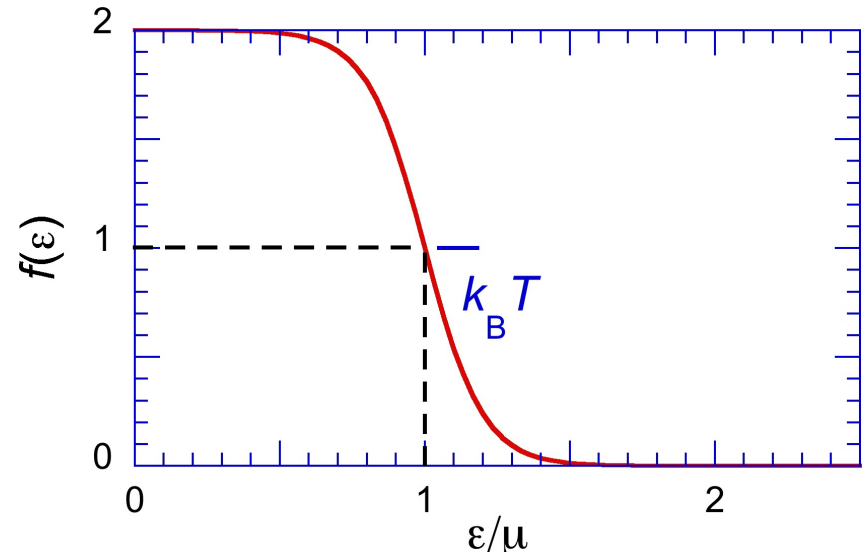
$$v(\mathbf{r}) = - \sum_I \frac{Z_I e^2}{|\mathbf{r} - \mathbf{R}_I|} + \int d\mathbf{r}' \frac{e^2 \rho(\mathbf{r}')}{|\mathbf{r} - \mathbf{r}'|} + v_{xc}(\mathbf{r})$$

$$\rho(\mathbf{r}) = \sum_n \frac{2}{\exp\left(\frac{\epsilon_n - \mu}{k_B T}\right) + 1} |\psi_n(\mathbf{r})|^2$$

exchange-correlation potential

\* $T = 0$  in Kohn-Sham'65; cf. Mermin

[Phy. Rev. 137, A1441 ('65)]



# Abstraction: Exchange-Correlation Functional

- Universal functional (of density) that describes many-body effects beyond the mean-field approximation

$$v_{\text{Hxc}}(\mathbf{r}) = \int d\mathbf{r}' \frac{e^2 \rho(\mathbf{r}')}{|\mathbf{r} - \mathbf{r}'|} + v_{\text{xc}}(\mathbf{r})$$

potential energy  
due to electron-electron  
interaction      Hartree (mean-field)  
potential      exchange-correlation  
potential

- Some commonly used exchange-correlation functionals

> GGA (generalized gradient approximation)

**PBE:** Perdew, Burke & Ernzerhof, *Phys. Rev. Lett.* **77**, 3865 ('96)

## > MetaGGA

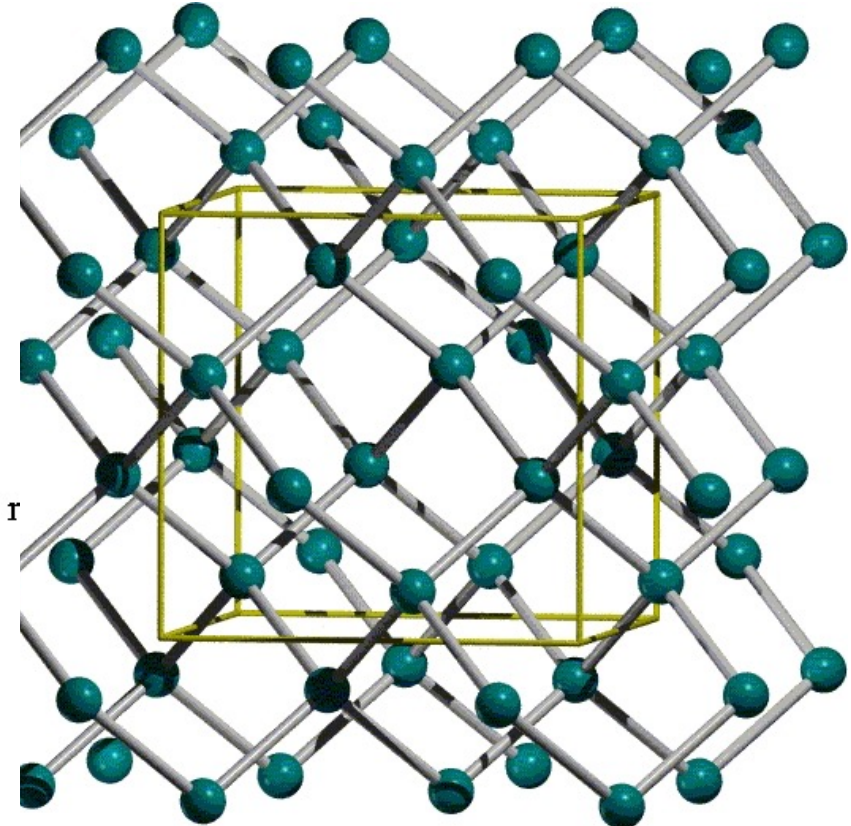
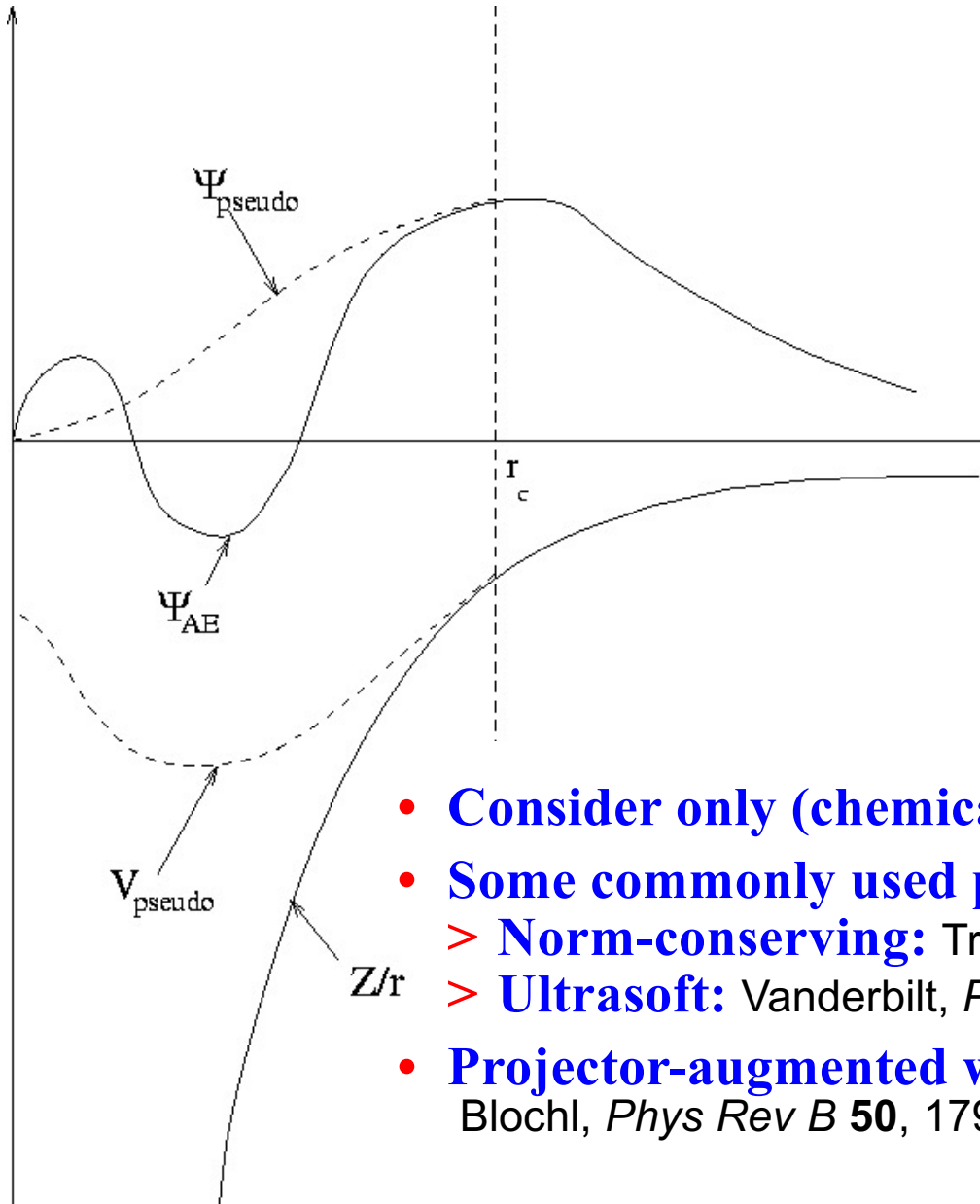
**SCAN:** Sun, Ruzsinszky & Perdew, *Phys. Rev. Lett.* **115**, 036402 ('15)

## > Hybrid exact-exchange (Hartree-Fock) functionals

**HSE:** Heyd, Scuseria & Ernzerhof, *J. Chem. Phys.* **118**, 8207 ('03)

# Abstraction: Pseudopotential

- Silicon —  $1s^2 2s^2 2p^6 3s^2 3p^2$



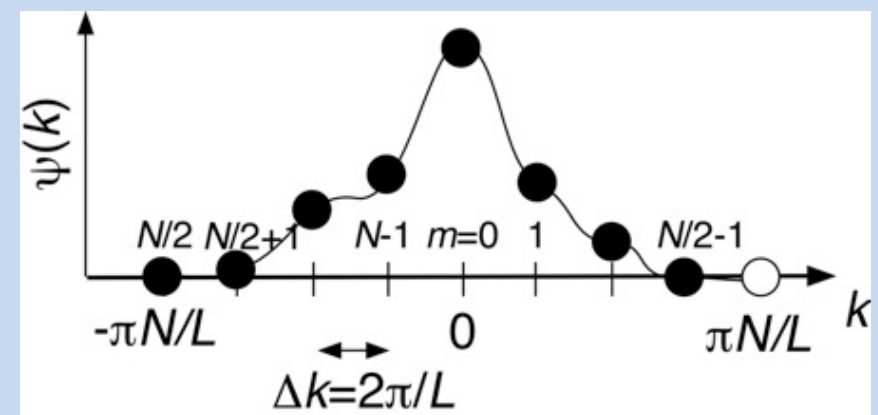
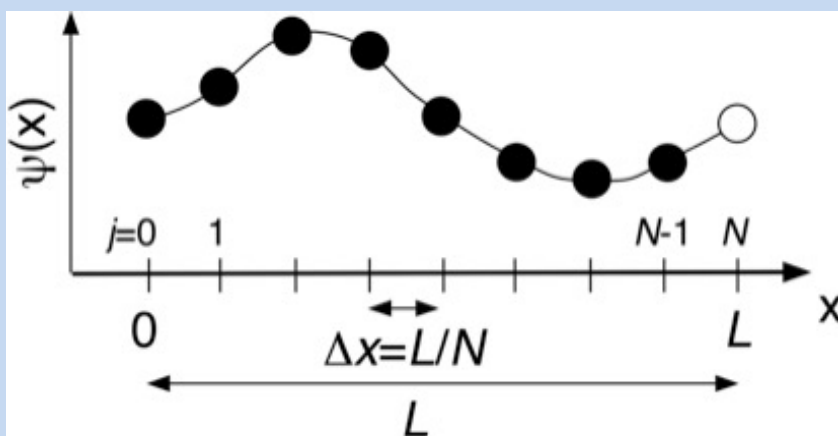
- Consider only (chemically active) valence electrons
- Some commonly used pseudopotentials
  - > Norm-conserving: Troullier & Martins, *Phys. Rev. B* **41**, 1993 ('91)
  - > Ultrasoft: Vanderbilt, *Phys. Rev. B* **41**, 7892 ('90)
- Projector-augmented wave (PAW) method  
Blochl, *Phys Rev B* **50**, 17953 ('94)

# Representation: Plane-Wave Basis

- Pseudopotentials result in slowly varying wave functions that can be represented on a regular grid, which in turn can be represented as a linear combination of plane waves, *i.e.*, Fourier transform

$$\psi(\mathbf{r}_j) = \sum_{\mathbf{k}_n} \psi_{\mathbf{k}_n} \exp(i \mathbf{k}_n \cdot \mathbf{r}_j)$$

1D example

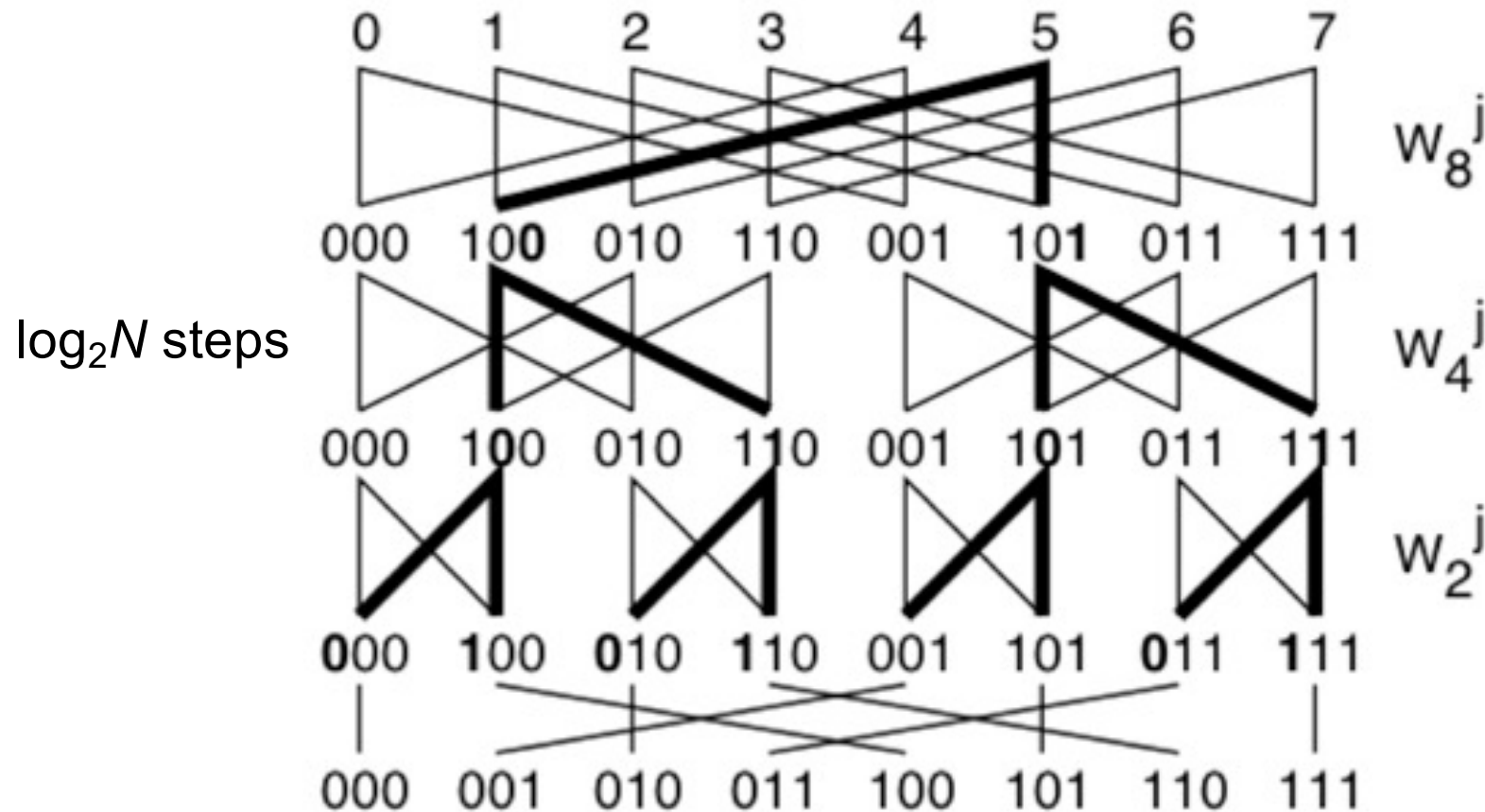


$$x_j = \frac{jL}{N}; \quad k_n = \frac{2\pi n}{L}$$

# Numerics: Fast Fourier Transform

- $O(N \log N)$  fast Fourier-transform (FFT) algorithm is typically used to perform Fourier transform

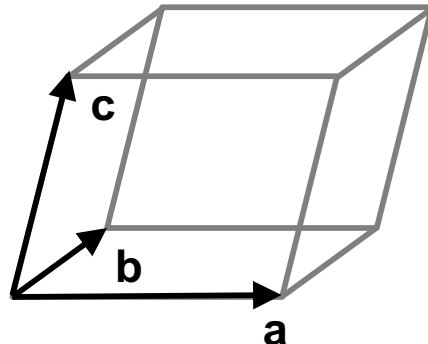
$$\psi(x_j) = \sum_{k_n} \psi_{k_n} \exp(i k_n x_j)$$



Butterfly (hypercube) data-exchange network

# Periodic Solid

- Consider a periodic solid with the unit cell spanned by vectors  $\mathbf{a}$ ,  $\mathbf{b}$  &  $\mathbf{c}$



- Fourier transform of a periodic function

$$u(\mathbf{r}) = \sum_{\mathbf{G}} u_{\mathbf{G}} \exp(i\mathbf{G} \cdot \mathbf{r})$$

$$\mathbf{G} = \frac{2\pi}{\mathbf{a} \cdot (\mathbf{b} \times \mathbf{c})} [l(\mathbf{b} \times \mathbf{c}), m(\mathbf{c} \times \mathbf{a}), n(\mathbf{a} \times \mathbf{b})] \quad (l, m, n \in \mathbb{Z})$$

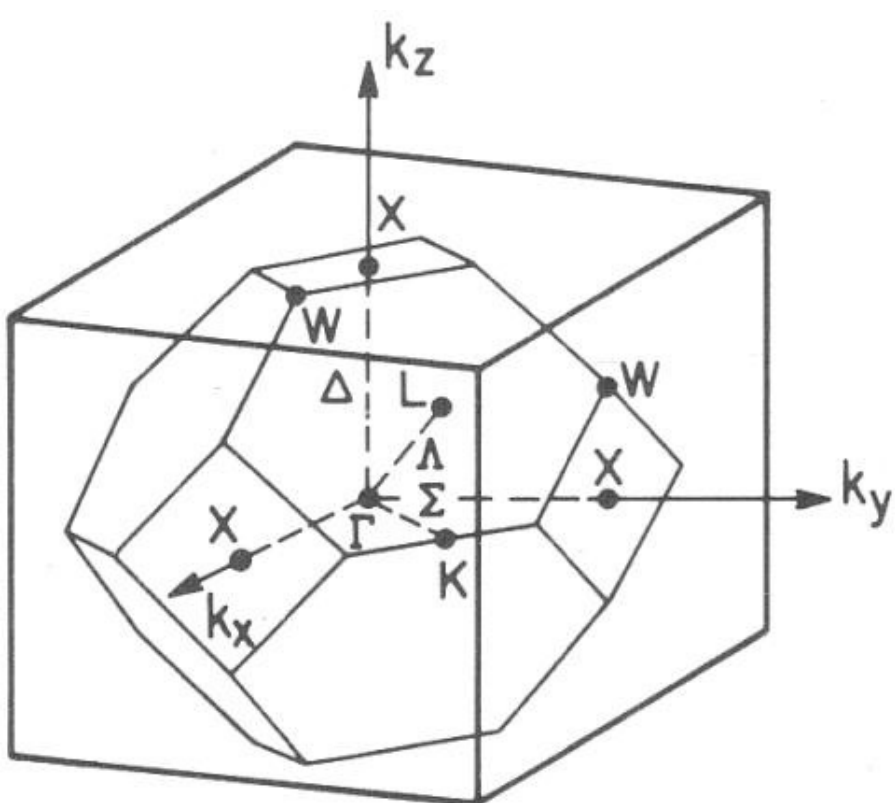
- Bloch's theorem

$$\begin{aligned} \psi_{n\mathbf{k}}(\mathbf{r}) &= \exp(i\mathbf{k} \cdot \mathbf{r}) u_{n,\mathbf{k}}(\mathbf{r}) \\ &= \sum_{\mathbf{G}} u_{n,\mathbf{k}}(\mathbf{G}) \exp(i(\mathbf{k} + \mathbf{G}) \cdot \mathbf{r}) \end{aligned}$$

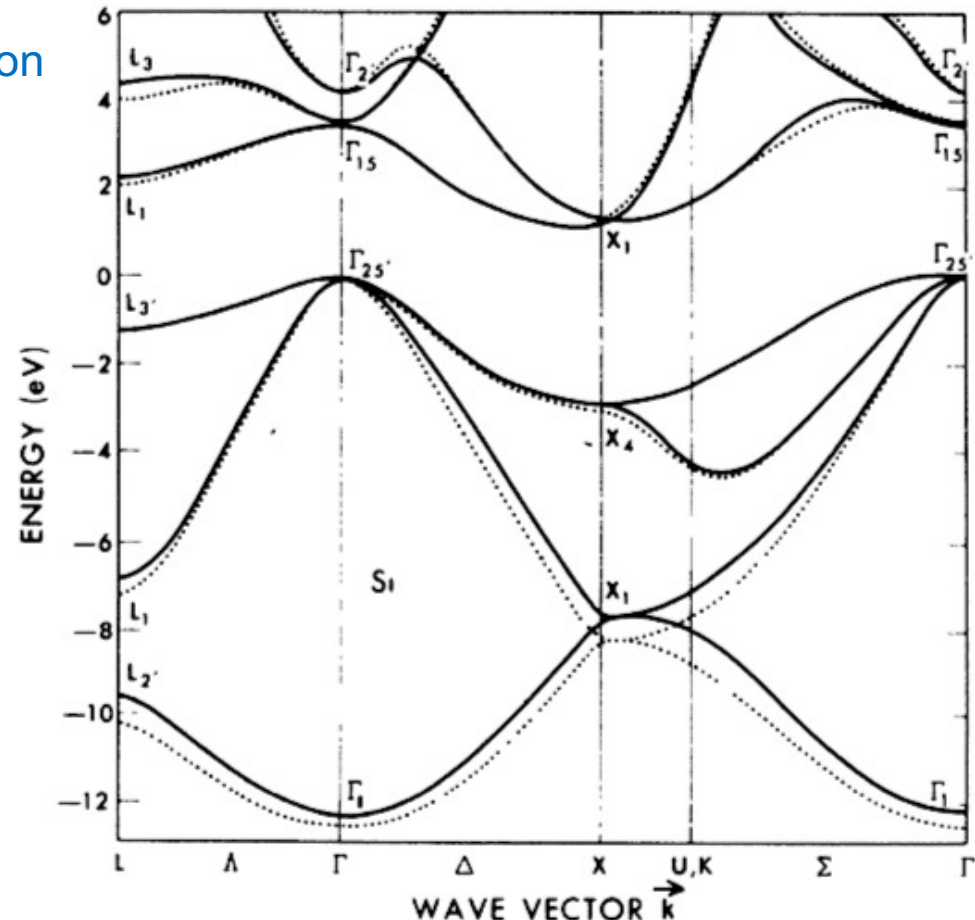
$\mathbf{k} \in$  first Brillouin zone in the reciprocal space

# Electronic Bands: Infinite Lattice

- **Bloch theorem:**  $\psi_{n\mathbf{k}}(\mathbf{r}) = \exp(i\mathbf{k} \cdot \mathbf{r})u_{n,\mathbf{k}}(\mathbf{r})$



Brillouin zone of Si crystal



Kohn-Sham energy

J. R. Chelikowsky & M. L. Cohen, *Phys. Rev. B* 10, 5095 ('74)

# Self-Consistent Field Iteration

$$\left( -\frac{\hbar^2}{2m} \frac{\partial^2}{\partial \mathbf{r}^2} + \hat{V}_{\text{ion}} + \hat{V}_{\text{H,xc}}[\rho(\mathbf{r})] \right) \psi_n(\mathbf{r}) = \epsilon_n \psi_n(\mathbf{r})$$

Given  $\rho(\mathbf{r})$ ,  
iteratively obtain  
 $\{\psi_n, \epsilon_n\}$ , e.g., by  
preconditioned  
conjugate gradient

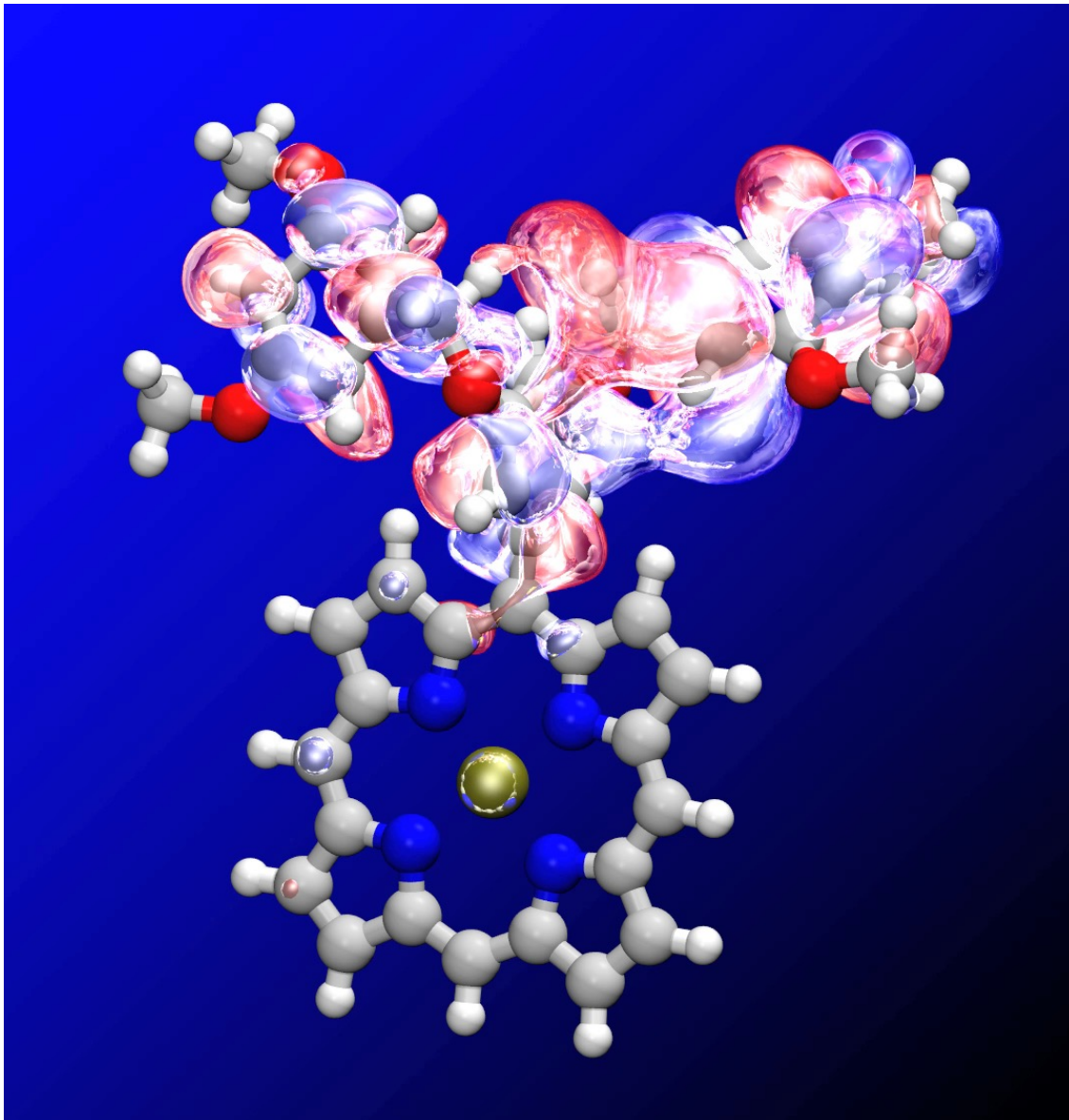
Given  $\{\psi_n, \epsilon_n\}$ ,  
determine  $\mu$  and  
compute  $\rho(\mathbf{r})$

$$\rho(\mathbf{r}) = \sum_n |\psi_n(\mathbf{r})|^2 \Theta(\mu - \epsilon_n)$$

Chemical potential

$$N = \int d\mathbf{r} \rho(\mathbf{r})$$

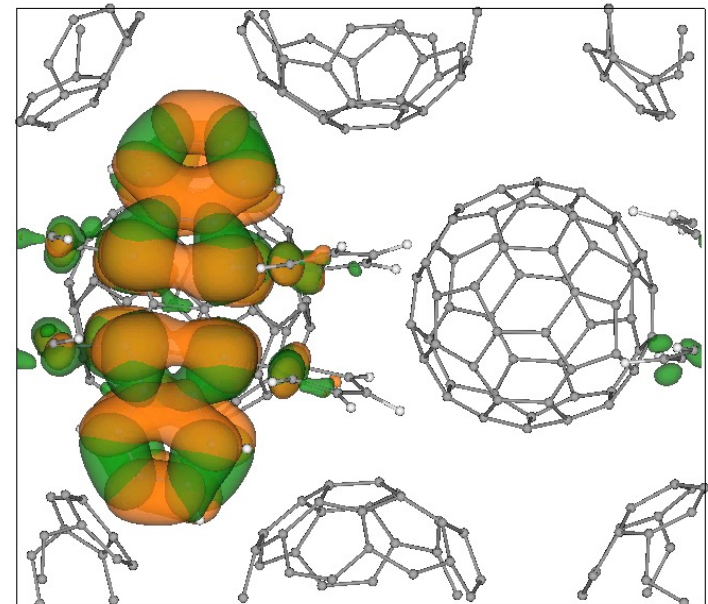
# Nonadiabatic Quantum Molecular Dynamics



W. Mou *et al.*, *Appl. Phys. Lett.* **98**, 113301 ('11);  
*ibid.* **100**, 203306 ('12); *J. Chem. Phys.* **136**,  
184705 ('12); *Comput. Phys. Commun.* **184**, 1  
('13); *Appl. Phys. Lett.* **102**, 093302 ('13); *ibid.*  
**102**, 173301 ('13); *J. Chem. Phys.* **140**, 18A529  
('14); *IEEE Computer* **48**(11), 33 ('15); *Sci. Rep.* **5**,  
19599 ('16); *Nature Commun.* **8**, 1745 ('17)

Zn porphyrin

Rubrene/C<sub>60</sub>



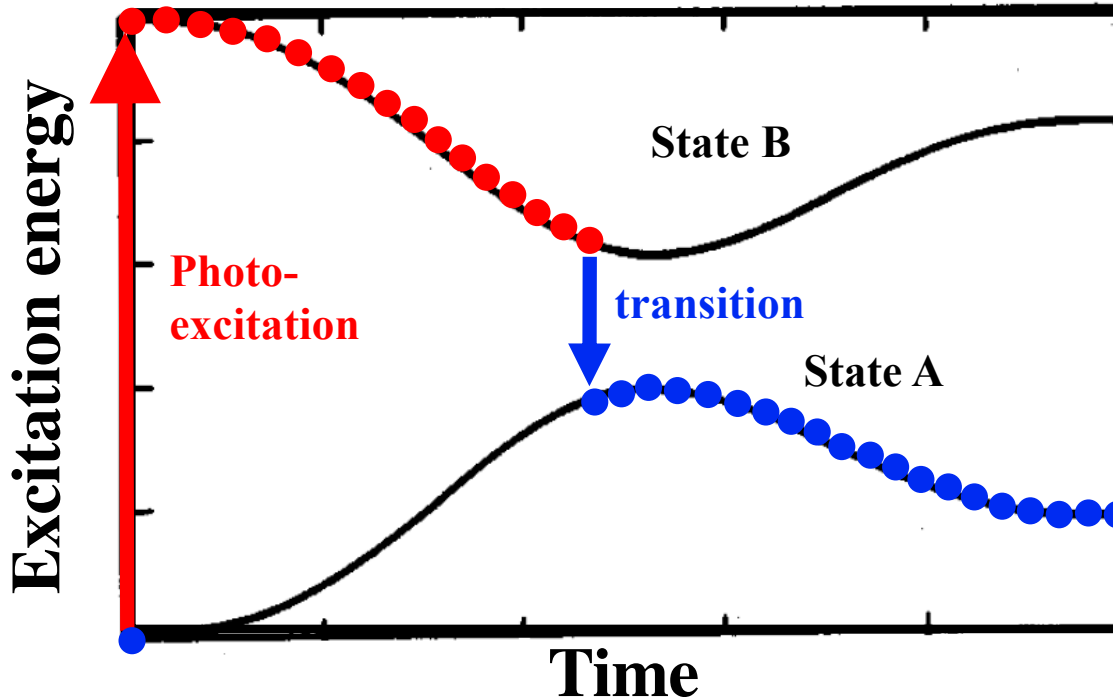
quasi-electron; quasi-hole

- **Excited states:** Linear-response time-dependent density functional theory [Casida, '95]
- **Interstate transitions:** Surface hopping [Tully, '90; Jaeger, Fisher & Prezhdo, '12]

# TDDFT & Surface Hopping

- Incorporate electron transitions with the time-dependent density-functional theory (TDDFT) & surface-hopping method

Tully, *J. Chem. Phys.* **93**, 1061 ('90); Craig et al., *Phys. Rev. Lett.* **95**, 163001 ('05)



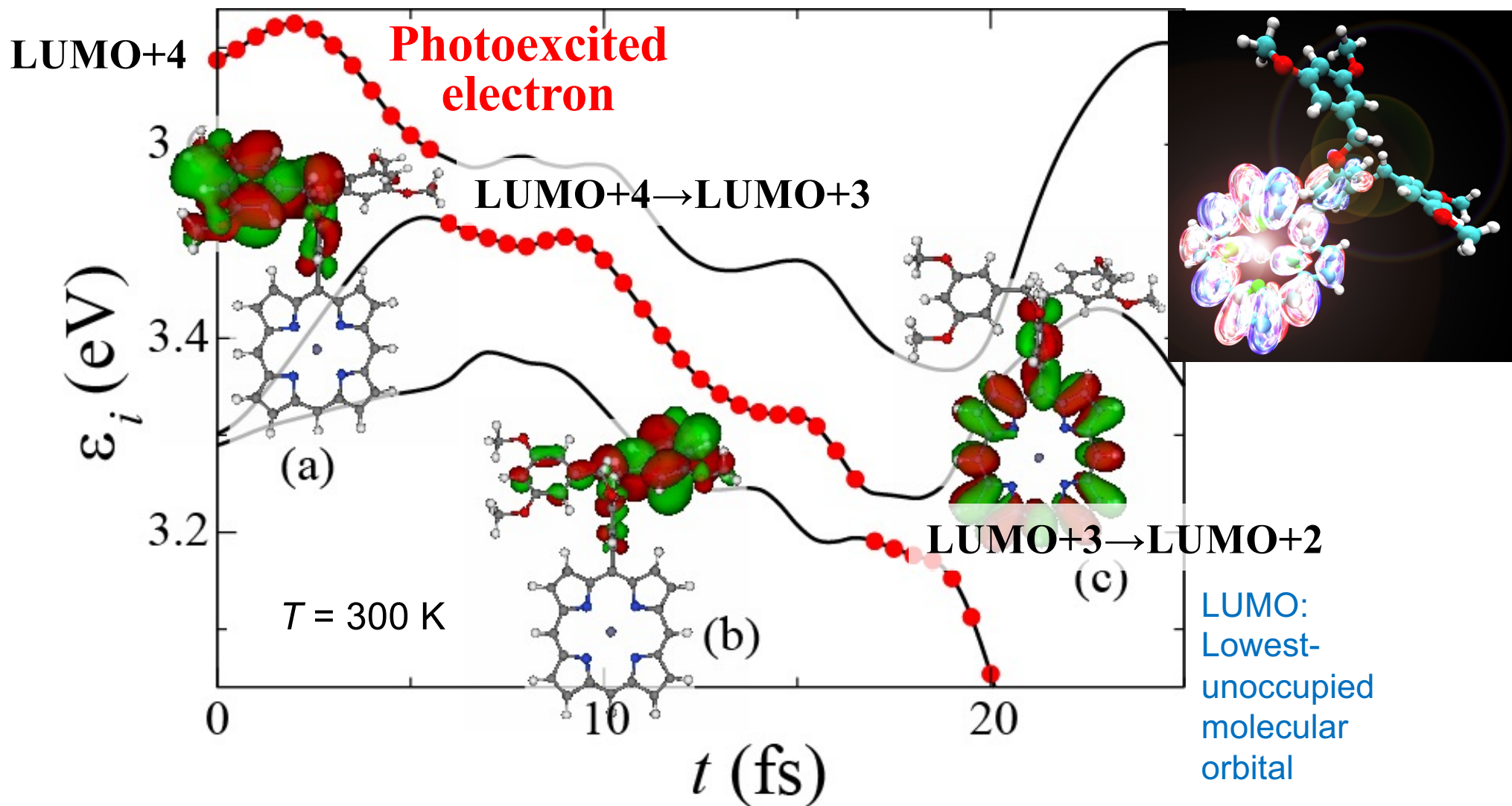
- Electronic transitions from the current state to another occur stochastically based on the switching probability obtained by solving TDDFT equations

$$\Psi(\mathbf{r}, t) = \sum_J C_J^{(I)}(t) \Phi_J(\mathbf{r}; \mathbf{R}(t)) \quad C_J^{(I)}(0) = \delta_{IJ}$$
$$\frac{d}{dt} C_J^{(I)}(t) = - \sum_k C_k^{(I)}(t) \left( i\omega_K \delta_{JK} + \langle \Phi_J | \frac{\partial}{\partial t} | \Phi_K \rangle \right)$$

Nonadiabatic coupling

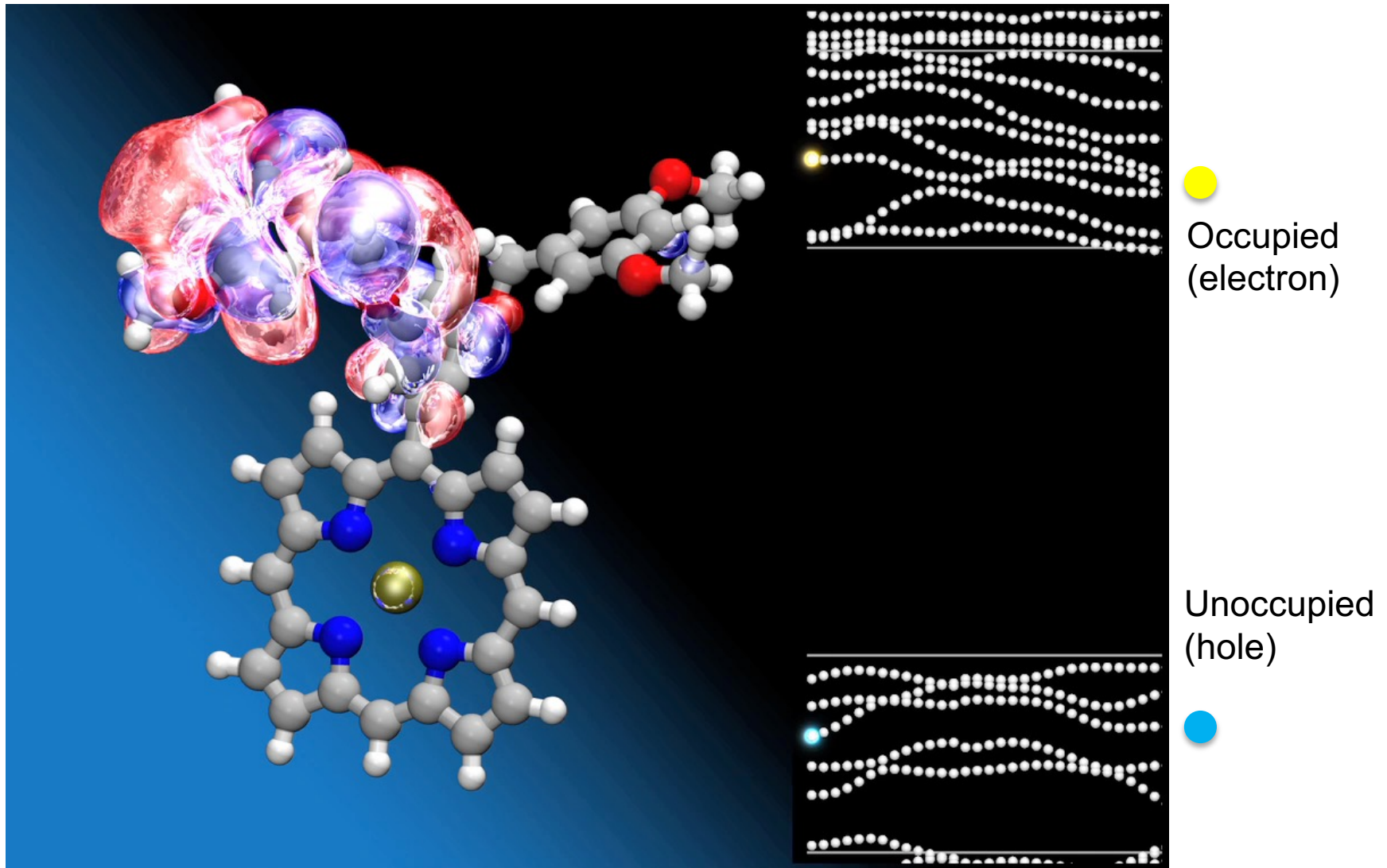
*J*-th adiabatic excited state  
*K*-th excitation frequency

# Example: Electron Transfer in a Dendrimer



- The photoexcited electron at the peripheral antenna is transferred to the core due to the energy-crossing & overlapping of orbitals assisted by thermal molecular motions

# Electron Transfer in a Light-Harvesting Dendrimer



- The photoexcited electron at the peripheral antenna is transferred to the core due to the energy-crossing & overlapping of orbitals assisted by thermal molecular motions

# Excitonic Effects: LR-TDDFT

- Excited electron-hole pairs within the linear-response time-dependent density functional theory (LR-TDDFT) [Casida, '95]

$$\delta V(t) = \delta v_{kl\tau}(t) \hat{a}_{k\tau}^+ \hat{a}_{l\tau} \longrightarrow \delta P_{ij\sigma}(t) = \delta \langle \Phi(t) | \hat{a}_{i\sigma}^+ \hat{a}_{j\sigma} | \Phi(t) \rangle$$

$$\chi_{ij\sigma,kl\tau}(t - t') = \delta P_{ij\sigma}(t) / \delta v_{kl\tau}(t')$$

electron    hole

- Excitation energies from the poles of the response function  $\chi_{ij\tau,klo}(\omega)$

$2N_{\text{unoccupied}} N_{\text{occupied}} \times 2N_{\text{unoccupied}} N_{\text{occupied}}$  matrix eigenequation

$$\begin{pmatrix} \mathbf{A} & \mathbf{B} \\ \mathbf{B}^* & \mathbf{A}^* \end{pmatrix} \begin{pmatrix} \mathbf{X}_I \\ \mathbf{Y}_I \end{pmatrix} = \hbar \omega_I \begin{pmatrix} 1 & 0 \\ 0 & -1 \end{pmatrix} \begin{pmatrix} \mathbf{X}_I \\ \mathbf{Y}_I \end{pmatrix}$$

*I-th excitation energy*

Kohn-Sham energy

$$A_{ia\sigma,jb\tau} = \delta_{\sigma,\tau} \delta_{i,j} \delta_{a,b} (\varepsilon_{a\sigma} - \varepsilon_{i\sigma}) + K_{ia\sigma,jb\tau} \quad B_{ia\sigma,jb\tau} = K_{ia\sigma,bj\tau}$$

$$K_{ia\sigma,i'a'\sigma'} = \iint \psi_{i\sigma}^*(\mathbf{r}) \psi_{a\sigma}(\mathbf{r}) \left( \frac{e^2}{|\mathbf{r} - \mathbf{r}'|} + \frac{\delta^2 E_{\text{xc}}}{\delta \rho_\sigma(\mathbf{r}) \delta \rho_{\sigma'}(\mathbf{r}')} \right) \psi_{i'\sigma'}^*(\mathbf{r}') \psi_{a'\sigma'}(\mathbf{r}') d\mathbf{r} d\mathbf{r}'$$

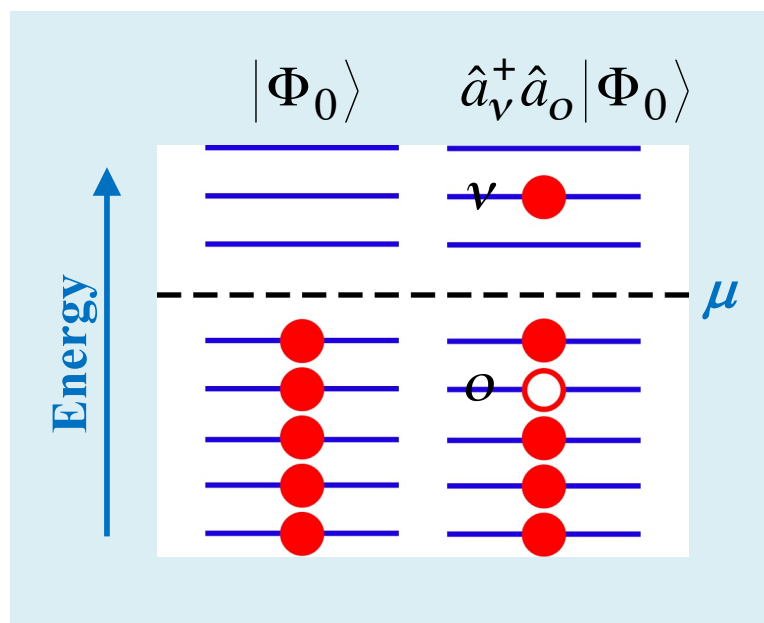
Coulomb & exchange-correlation interaction matrix elements

# Electronic Excited States

- $I$ -th excited state

$$|\Phi_I(\mathbf{r}; \mathbf{R})\rangle = \sum_{i \in \{\text{occupied}\}} \sum_{a \in \{\text{unoccupied}\}} \sum_{\sigma} \sqrt{\frac{\varepsilon_{a\sigma} - \varepsilon_{i\sigma}}{\hbar\omega_I}} (X_{I,ia\sigma} + Y_{I,ia\sigma}) \hat{a}_{a\sigma}^+ \hat{a}_{i\sigma} |\Phi_0(\mathbf{r}; \mathbf{R})\rangle$$

electron-hole pair      ground state



# QXMD Code

---

- Quantum molecular dynamics (**QMD**) code developed by Prof. Fuyuki Shimojo at Kumamoto University in Japan
- Various eXtensions co-developed with USC-CACS: Nonadiabatic QMD, linear-scaling divide-&-conquer, parallelization, *etc.*
- Unique features:
  - > Interatomic forces with electronic excitation to study photo-excited lattice dynamics  
Shimojo *et al.*, *Comput. Phys. Commun.* **184**, 1 ('13)
  - > Range-separated hybrid exact-exchange functional for exciton binding  
Tawada *et al.*, *J. Chem. Phys.* **120**, 8425 ('04)
  - > Lean divide-&-conquer density functional theory (LDF-DFT) with small  $O(N)$  prefactor  
Shimojo *et al.*, *J. Chem. Phys.* **140**, 18A529 ('14)
  - > Omni-directional multiscale shock technique (OD-MSST)  
Shimamura *et al.*, *Appl. Phys. Lett.* **107**, 231903 ('15); **108**, 071901 ('16)
  - > Berry-phase computation of bulk polarization
- Other features:
  - > Various functionals: spin-polarized, GGA+U, DFT+D, nonlocal correlation
  - > Nudged elastic band (NEB) method for energy-barrier calculation

**GitHub repository:**

[https://github.com/USCCACS/QXMD\\_Course](https://github.com/USCCACS/QXMD_Course)

**Software download site:**

<https://magics.usc.edu/qxmd>

# Current & Future Computing Platforms

- Won two DOE supercomputing awards to develop & deploy metascalable (“design once, scale on future platforms”) simulation algorithms (2017-2020)



## Innovative & Novel Computational Impact on Theory & Experiment

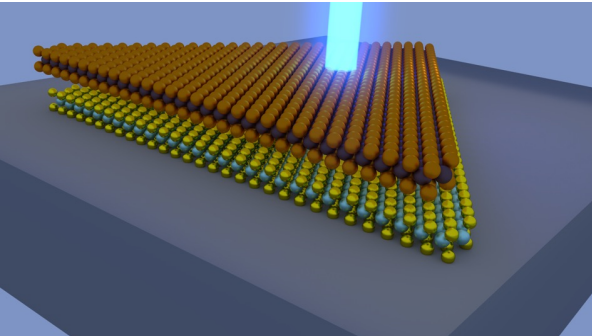
**Title:** “Petascale Simulations for Layered Materials Genome”

**Principal Investigator:**

**Co-Investigator:**

Aiichiro Nakano, University of Southern California

Priya Vashishta, University of Southern California



Early Science Projects for Aurora

Supercomputer Announced

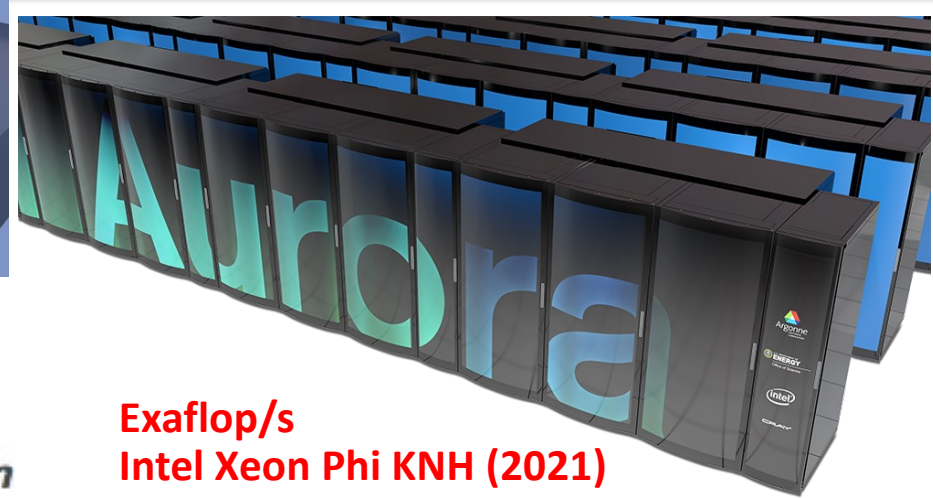
**Metascalable layered materials genome**

**Investigator: Aiichiro Nakano, University of Southern California**

- One of 10 exclusive users of the next-generation DOE supercomputer



**786,432-core IBM Blue Gene/Q**



**Exaflop/s  
Intel Xeon Phi KNH (2021)**

# But...



## Intel Dumps Knights Hill, Future of Xeon Phi Product Line Uncertain

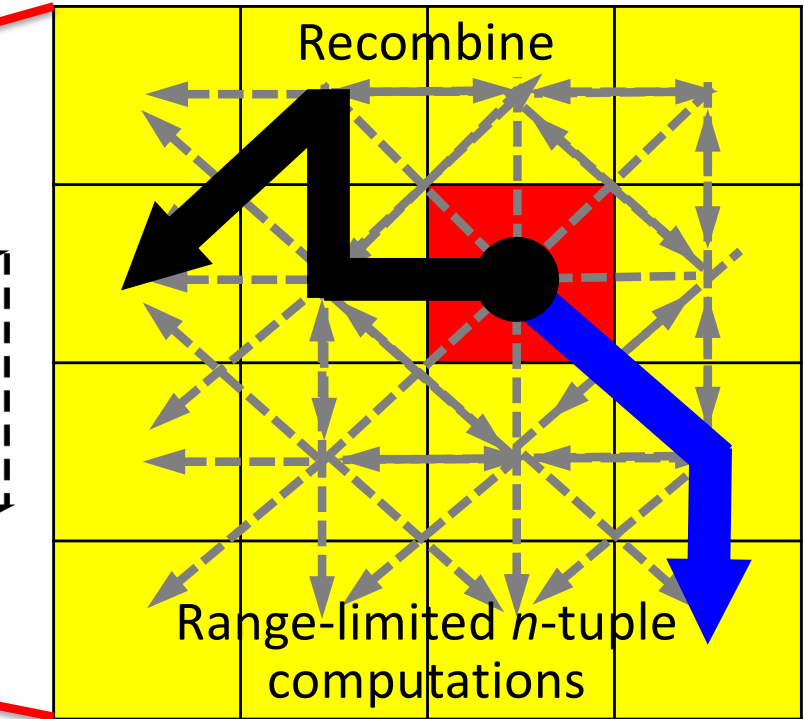
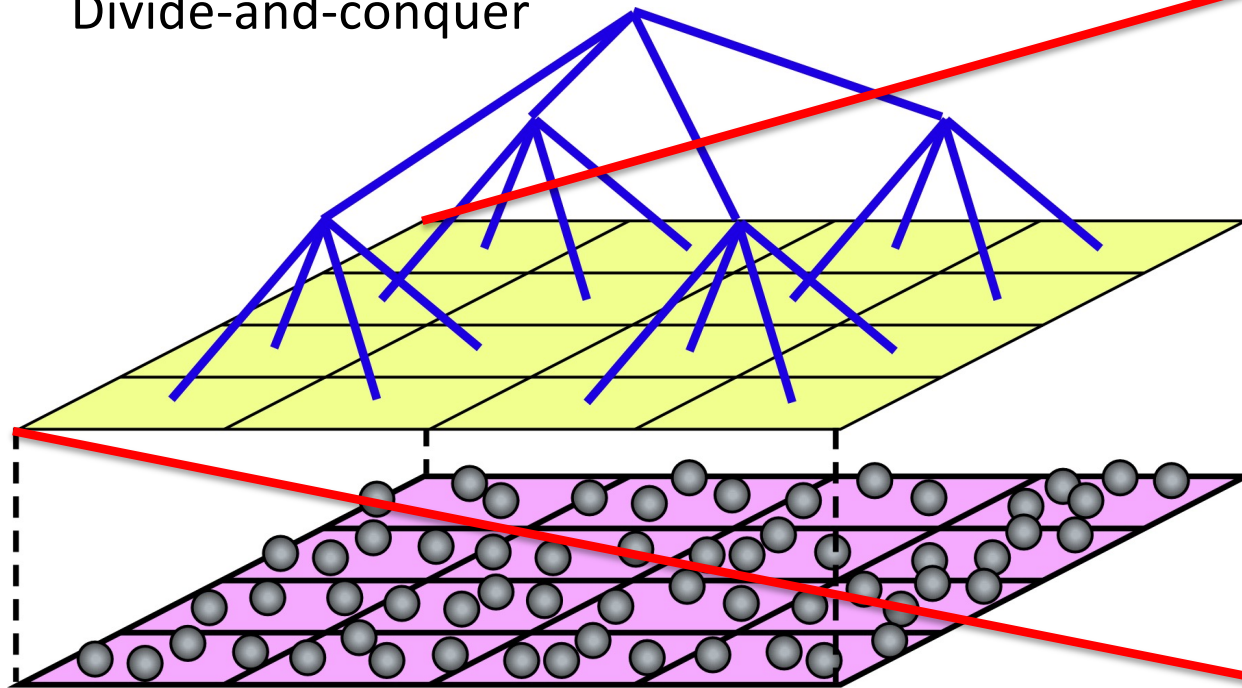
Michael Feldman | November 15, 2017 04:34 CET

<https://www.top500.org/news/>

- Need *metascalable* (or “design once, scale on new architectures”) parallel applications
- Proposed *divide-conquer-recombine*

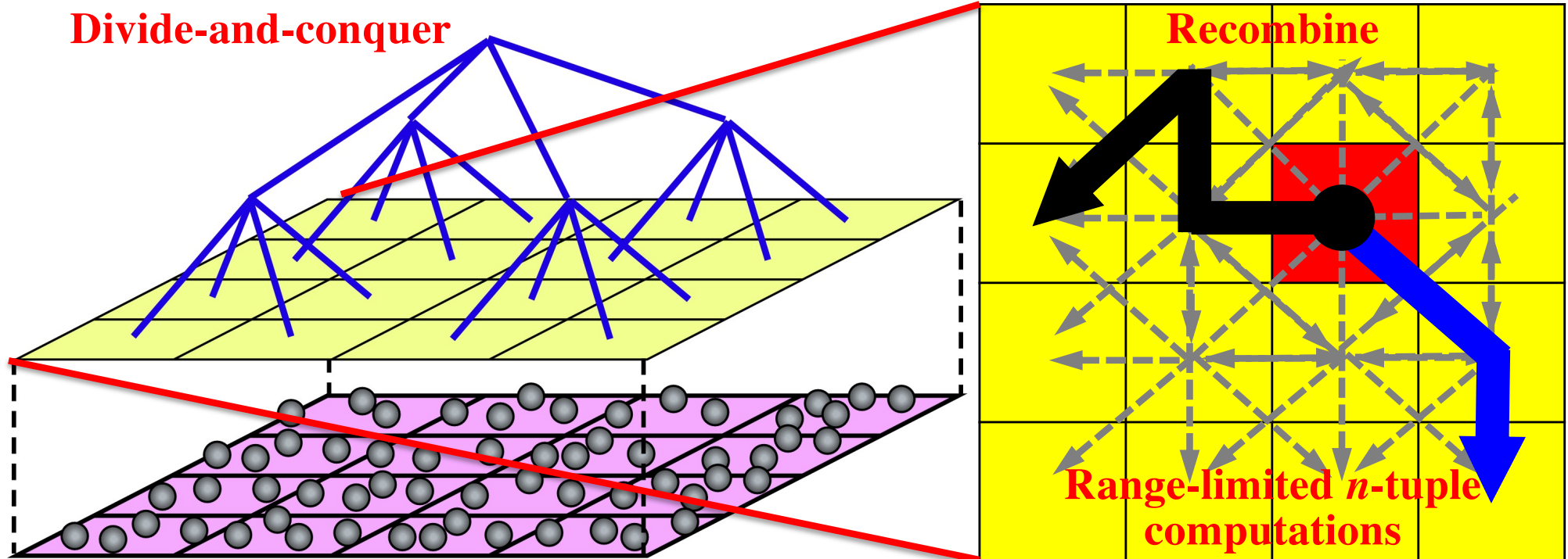
F. Shimojo *et al.*, *J. Chem. Phys.* **140**, 18A529 ('14);  
K. Nomura *et al.*, *ACM/IEEE SC14* ('14)

Divide-and-conquer



M. Kunaseth *et al.*, *ACM/IEEE SC13* ('13)

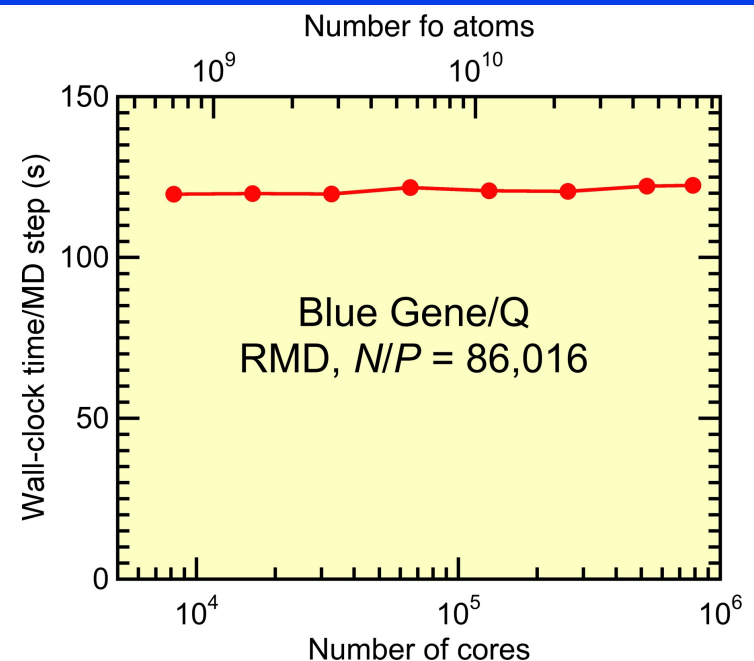
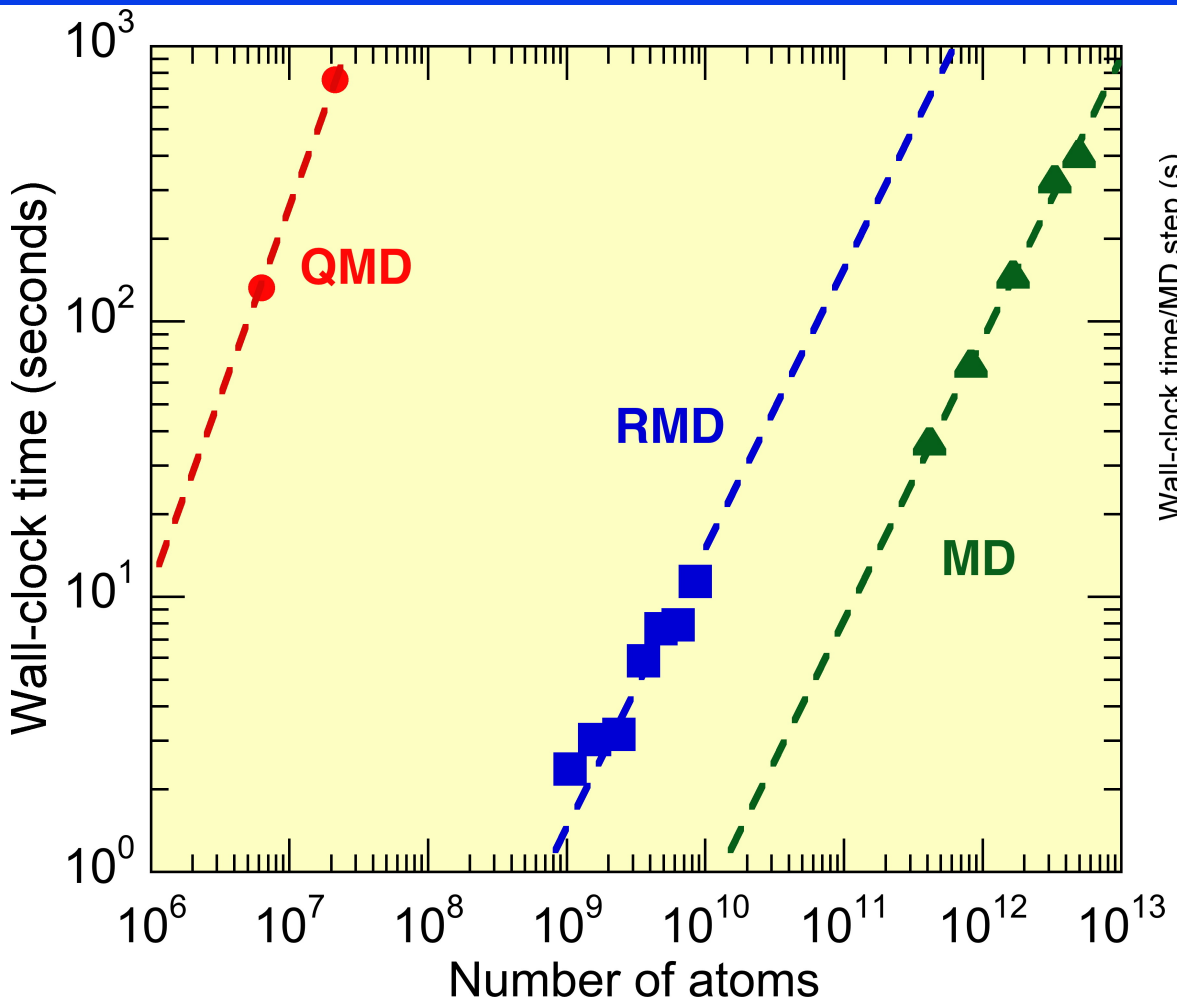
# Divide-Conquer-Recombine (DCR) Engines



M. Kunaseth et al., ACM/IEEE SC13

- **Quantum MD:** Lean divide-&-conquer density functional theory (LDC-DFT) algorithm minimizes the prefactor of  $O(N)$  computational cost  
F. Shimojo et al., *J. Chem. Phys.* **140**, 18A529 ('14); K. Nomura et al., *IEEE/ACM SC14*
- **Reactive MD:** Extended-Lagrangian reactive molecular dynamics (XRMD) algorithm eliminates the speed-limiting charge iteration  
K. Nomura et al., *Comput. Phys. Commun.* **192**, 91 ('15)

# Scalable Simulation Algorithm Suite



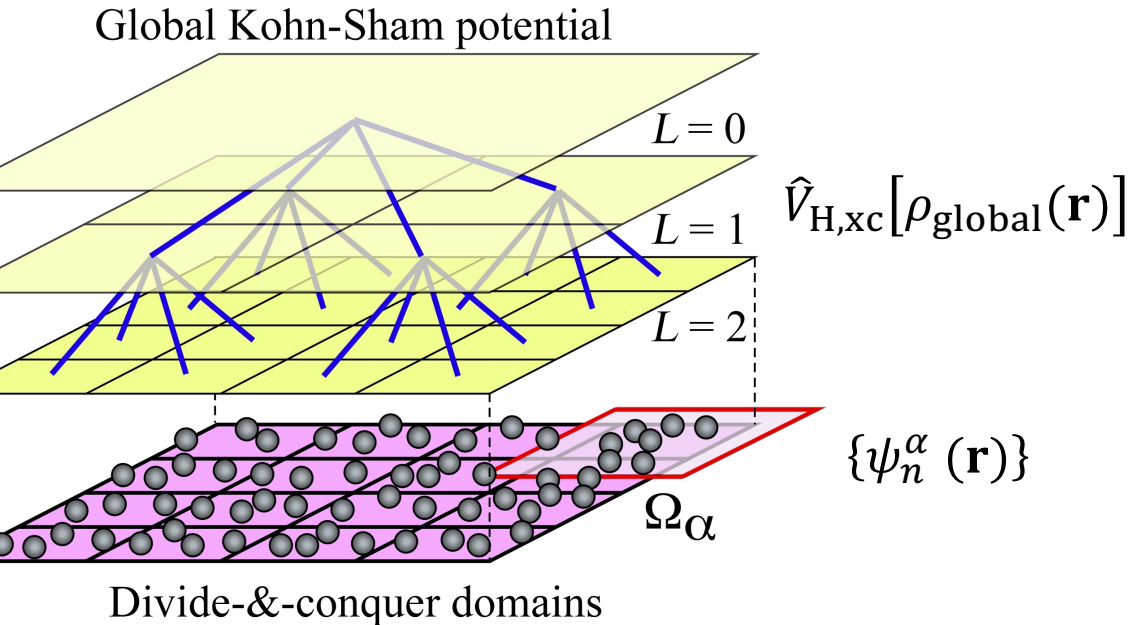
**QMD (quantum molecular dynamics): DC-DFT**

**RMD (reactive molecular dynamics): F-ReaxFF**

**MD (molecular dynamics): MRMD**

- 4.9 trillion-atom space-time multiresolution MD (MRMD) of  $\text{SiO}_2$
  - 67.6 billion-atom fast reactive force-field (F-ReaxFF) RMD of RDX
  - 39.8 trillion grid points (50.3 million-atom) DC-DFT QMD of SiC
- parallel efficiency 0.984 on 786,432 Blue Gene/Q cores

# Divide-&-Conquer Density Functional Theory



- Overlapping spatial domains:  $\Omega = \bigcup_\alpha \Omega_\alpha$
- Domain Kohn-Sham equations

Global-local  
self-consistent  
field (SCF)  
iteration

$$\left( -\frac{1}{2} \nabla^2 + \hat{V}_{\text{ion}} + \hat{V}_{\text{H,xc}}[\rho_{\text{global}}(\mathbf{r})] \right) \psi_n^\alpha(\mathbf{r}) = \epsilon_n^\alpha \psi_n^\alpha(\mathbf{r})$$

- Global & domain electron densities

$$\rho_{\text{global}}(\mathbf{r}) = \sum_\alpha p_\alpha(\mathbf{r}) \rho_\alpha(\mathbf{r}) \quad \rho_\alpha(\mathbf{r}) = \sum_n [\psi_n^\alpha]^2 \Theta(\mu - \epsilon_n^\alpha)$$

Domain support function

$$\sum_\alpha p_\alpha(\mathbf{r}) = 1$$

Global chemical potential

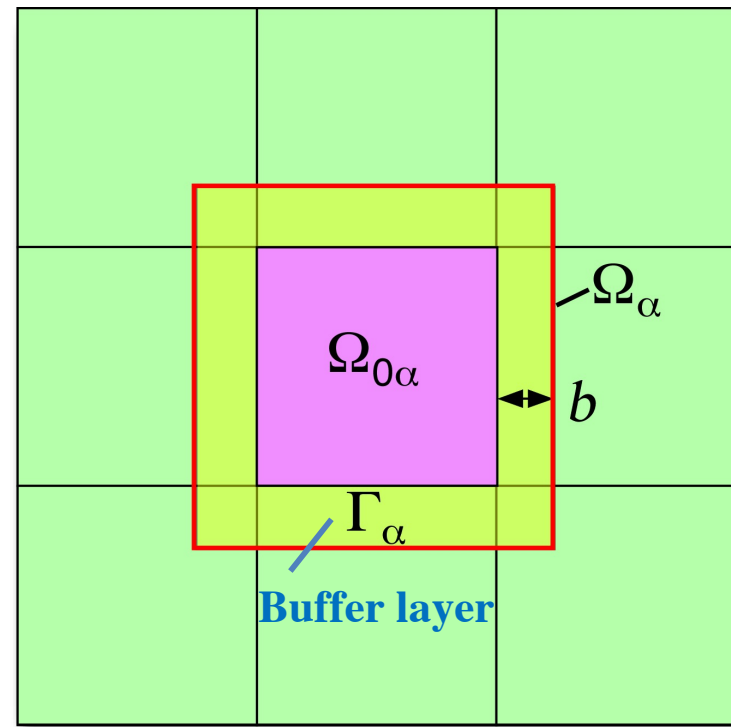
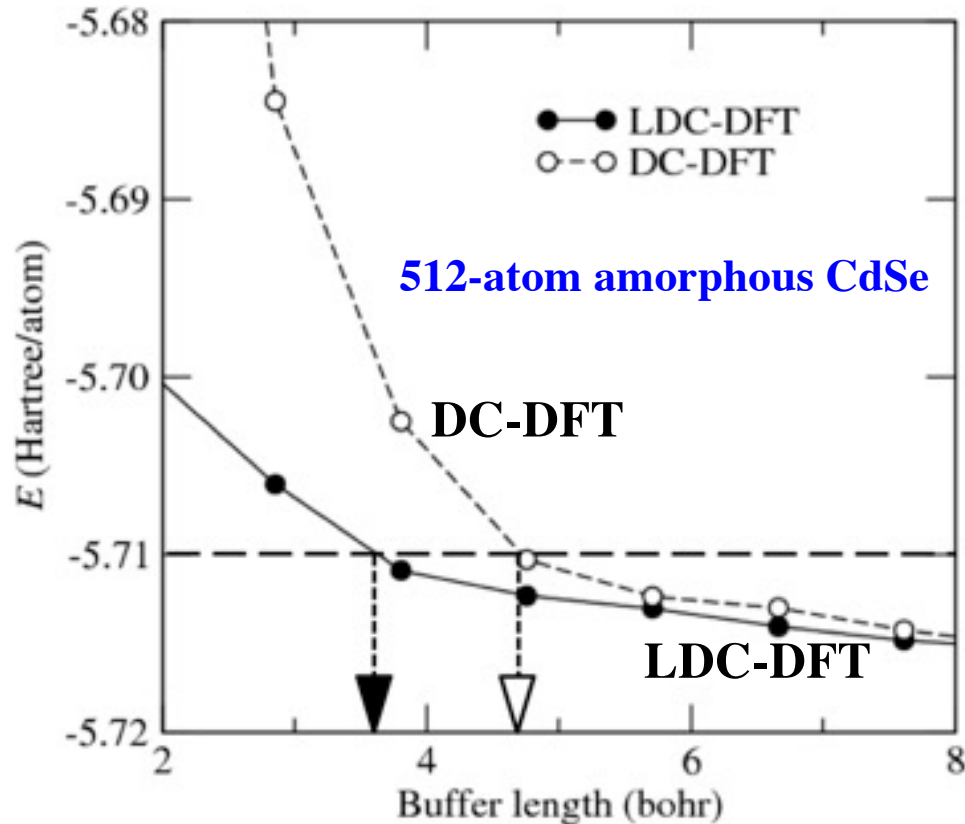
$$N = \int d\mathbf{r} \rho_{\text{global}}(\mathbf{r})$$

# Lean Divide-&-Conquer (LDC) DFT

- Density-adaptive boundary potential to reduce the  $O(N)$  prefactor

$$\nu_{\alpha}^{\text{bc}}(\mathbf{r}) = \int d\mathbf{r}' \frac{\partial \nu(\mathbf{r}')}{\partial \rho(\mathbf{r}')} (\rho_{\alpha}(\mathbf{r}') - \rho_{\text{global}}(\mathbf{r}')) \cong \frac{\rho_{\alpha}(\mathbf{r}) - \rho_{\text{global}}(\mathbf{r})}{\xi}$$

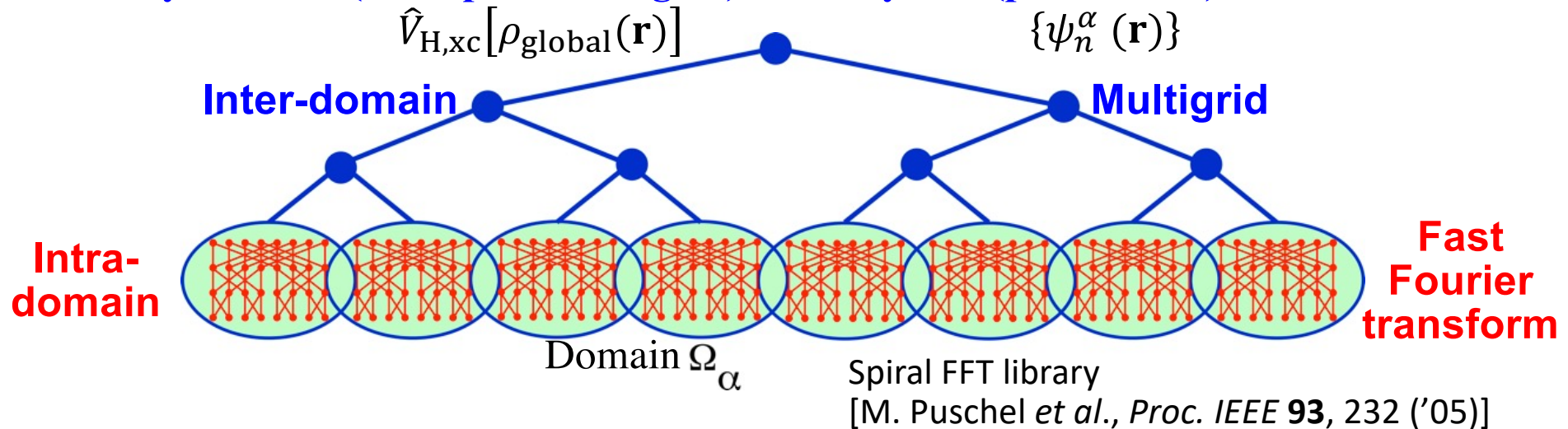
- More rapid energy convergence of LDC-DFT compared with nonadaptive DC-DFT



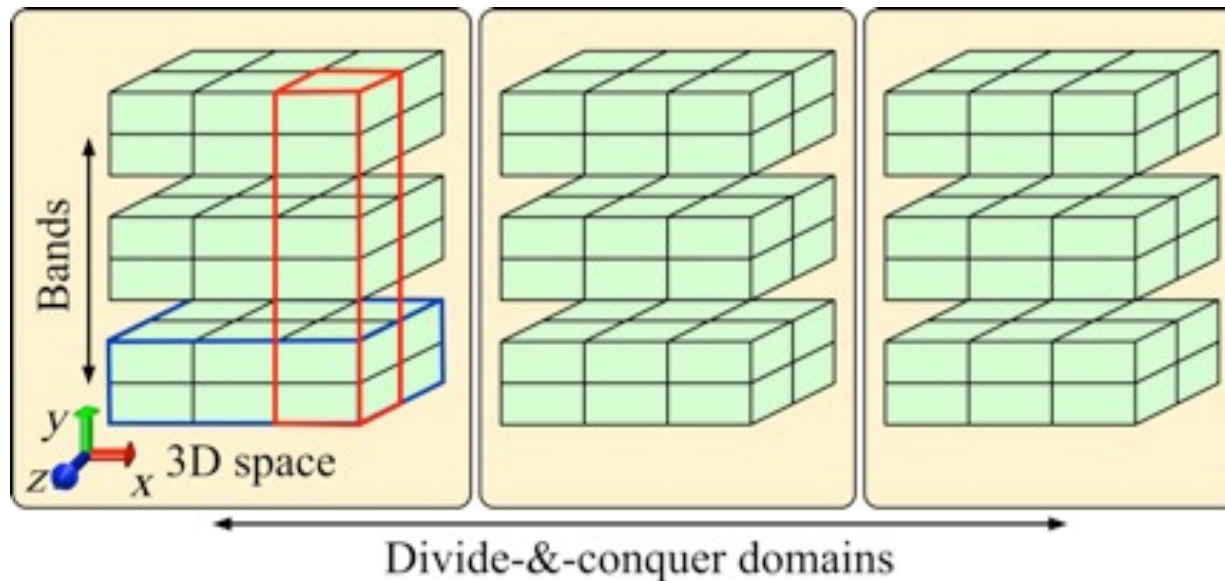
- Factor 2.03 (for  $\nu = 2$ )  $\sim 2.89$  (for  $\nu = 3$ ) reduction of the computational cost with an error tolerance of  $5 \times 10^{-3}$  a.u. (per-domain complexity:  $n^{\nu}$ )

# Hierarchical Computing

- Globally scalable (real-space multigrid) + locally fast (plane wave) electronic solver

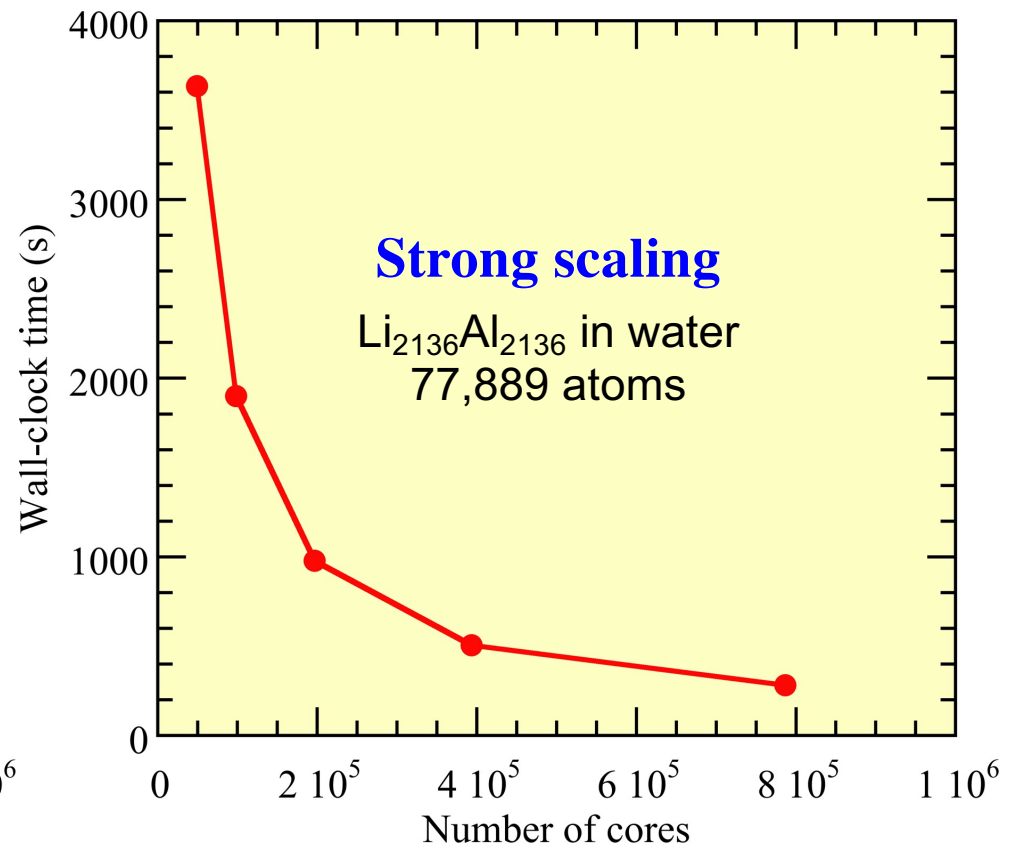
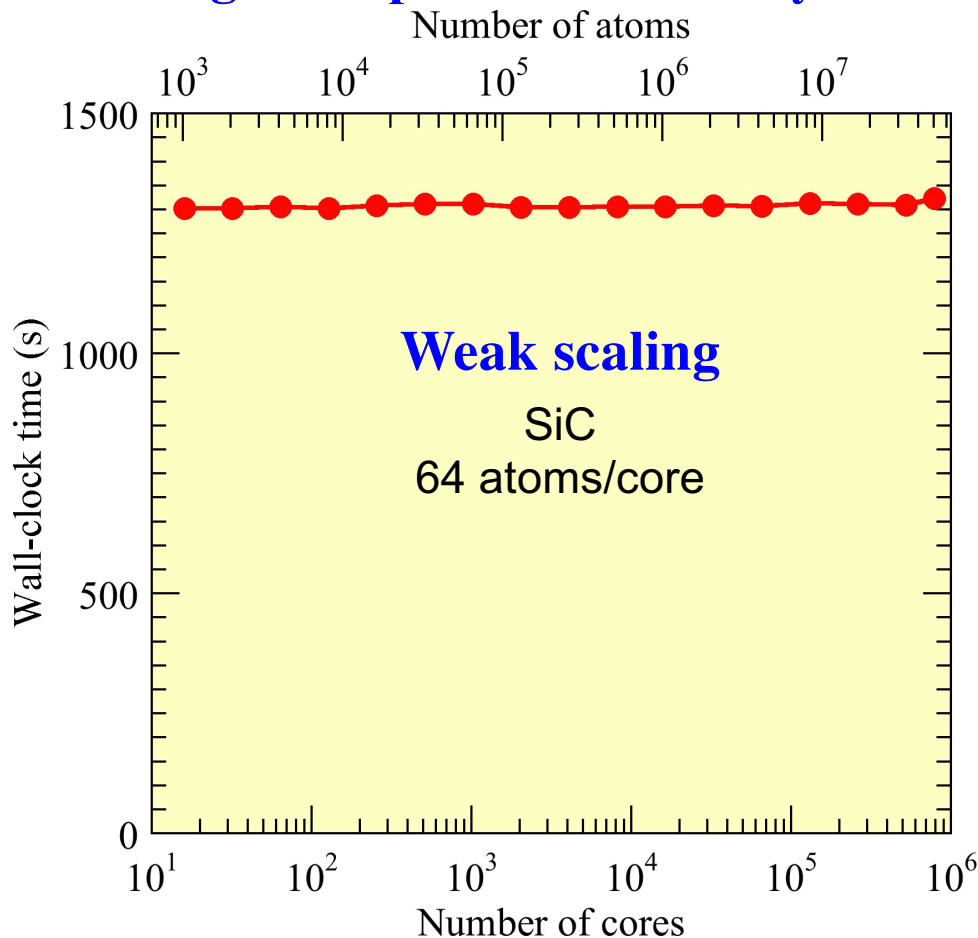


- Hierarchical band (*i.e.* Kohn-Sham orbital) + space + domain (BSD) decomposition



# Parallel Performance

- Weak-scaling parallel efficiency is 0.984 on 786,432 Blue Gene/Q cores for a 50,331,648-atom SiC system
- Strong-scale parallel efficiency is 0.803 on 786,432 Blue Gene/Q cores



- 62-fold reduction of time-to-solution [441 s/SCF-step for 50.3M atoms] from the previous state-of-the-art [55 s/SCF-step for 102K atoms, Osei-Kuffuor *et al.*, PRL '14]

# Floating Point Performance

- Transform from band-by-band to all-band computations to utilize a matrix-matrix subroutine (DGEMM) in the level 3 basic linear algebra subprograms (BLAS3) library
- Algebraic transformation of computations

## Example: Nonlocal pseudopotential operation

D. Vanderbilt, *Phys. Rev. B* **41**, 7892 ('90)

$$\hat{v}_{\text{nl}}|\psi_n^\alpha\rangle = \sum_I^{N_{\text{atom}}} \sum_{ij}^{L_{\max}} |\beta_{i,I}\rangle D_{ij,I} \langle \beta_{j,I}| \psi_n^\alpha \rangle \quad (n = 1, \dots, N_{\text{band}})$$



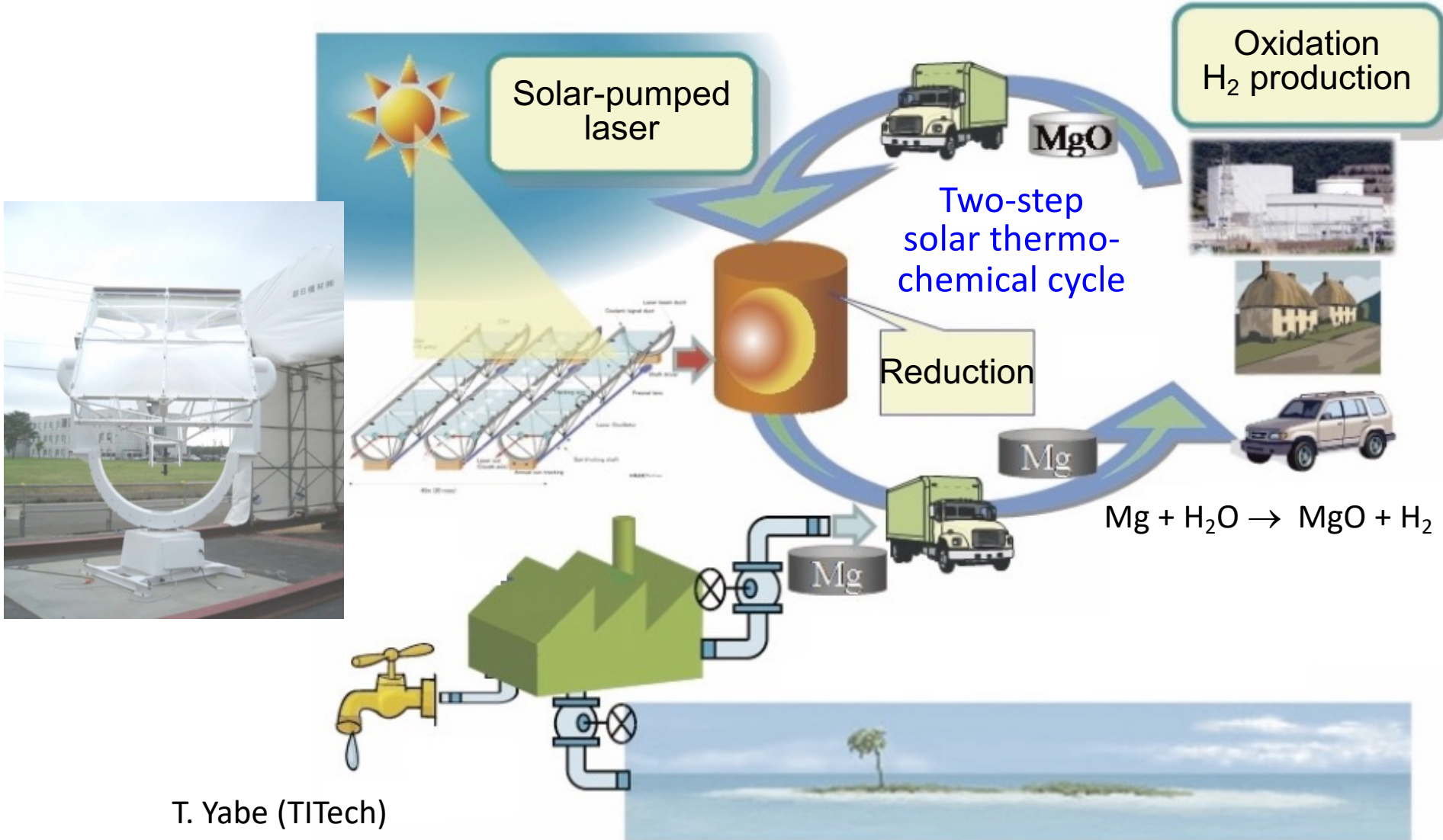
$$\Psi = [|\psi_1^\alpha\rangle, \dots, |\psi_{N_{\text{band}}}^\alpha\rangle] \quad \widetilde{\mathbf{B}}(i) = [|\beta_{i,1}\rangle, \dots, |\beta_{i,N_{\text{atom}}}\rangle] \quad [\widetilde{\mathbf{D}}(i,j)]_{I,J} = D_{ij,I} \delta_{IJ}$$

$$\hat{v}_{\text{nl}}\Psi = \sum_{i,j}^L \widetilde{\mathbf{B}}(i) \widetilde{\mathbf{D}}(i,j) \widetilde{\mathbf{B}}(j)^T$$

- **50.5% of the theoretical peak FLOP/s performance on 786,432 Blue Gene/Q cores (entire Mira at the Argonne Leadership Computing Facility)**
- **55% of the theoretical peak FLOP/s on Intel Xeon E5-2665**

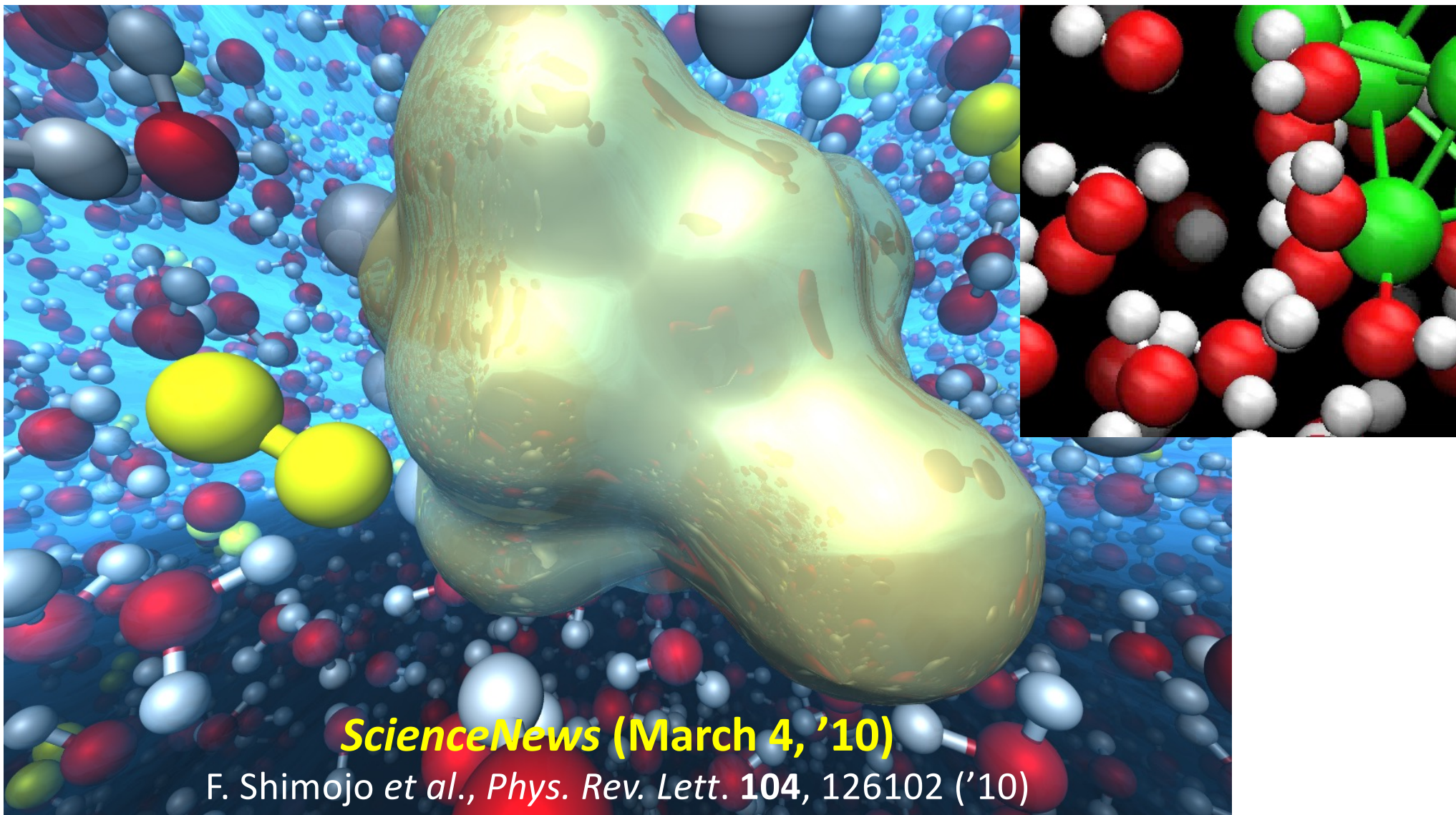
K. Nomura *et al.*, *IEEE/ACM Supercomputing, SC14* ('14)

# Renewal Energy Cycle by Metal Carriers



- **Problem: Accelerated hydrogen-production reaction kinetics for metal (Mg, Al, Zn, Fe) + water?**

# Nanotechnology Solution



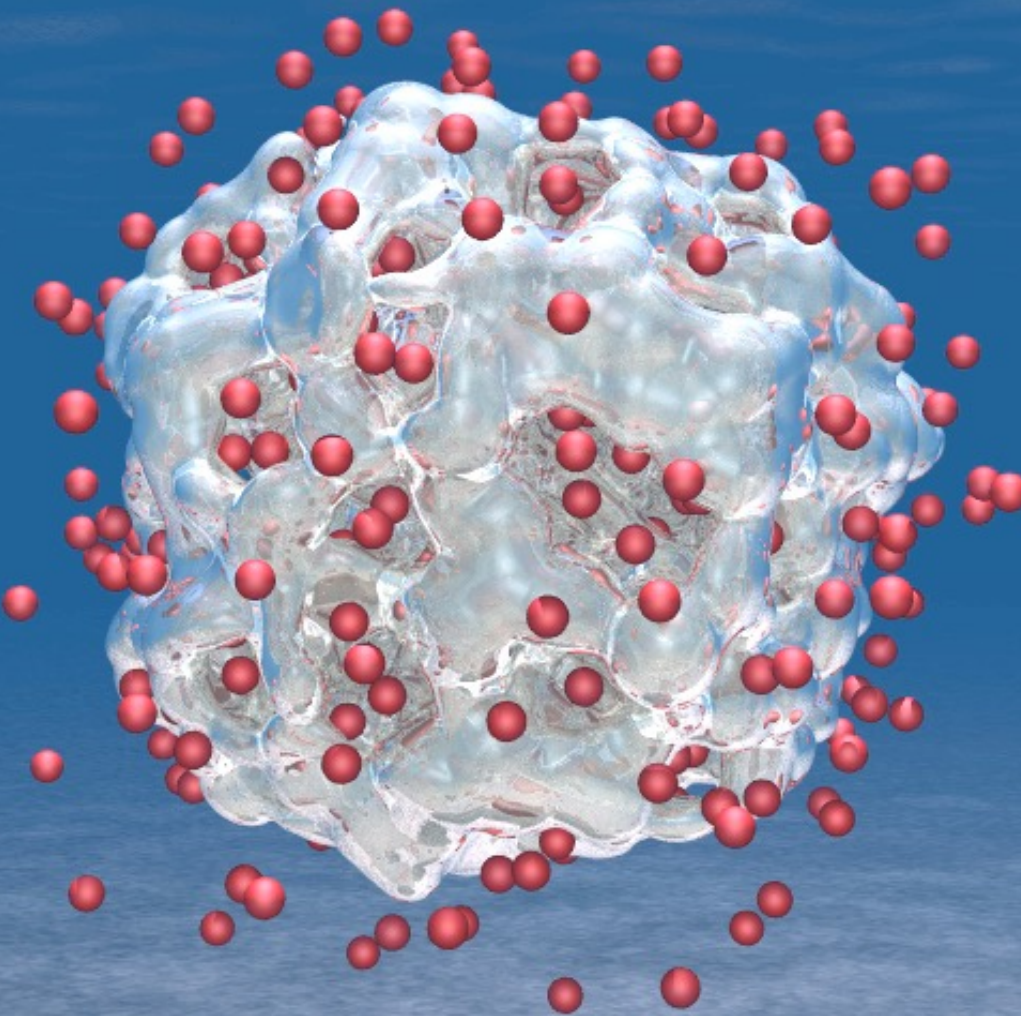
- QMD simulation shows rapid H<sub>2</sub> production from water by a superatom\* (Al<sub>17</sub>), but the technology is not scalable to larger particle sizes

\*Roach, Castleman, Khanna *et al.*, *Science* **323**, 492 ('09)

# H<sub>2</sub> Production from Water Using LiAl Particles

16,661-atom QMD simulation of Li<sub>441</sub>Al<sub>441</sub> in water  
on 786,432 IBM Blue Gene/Q cores

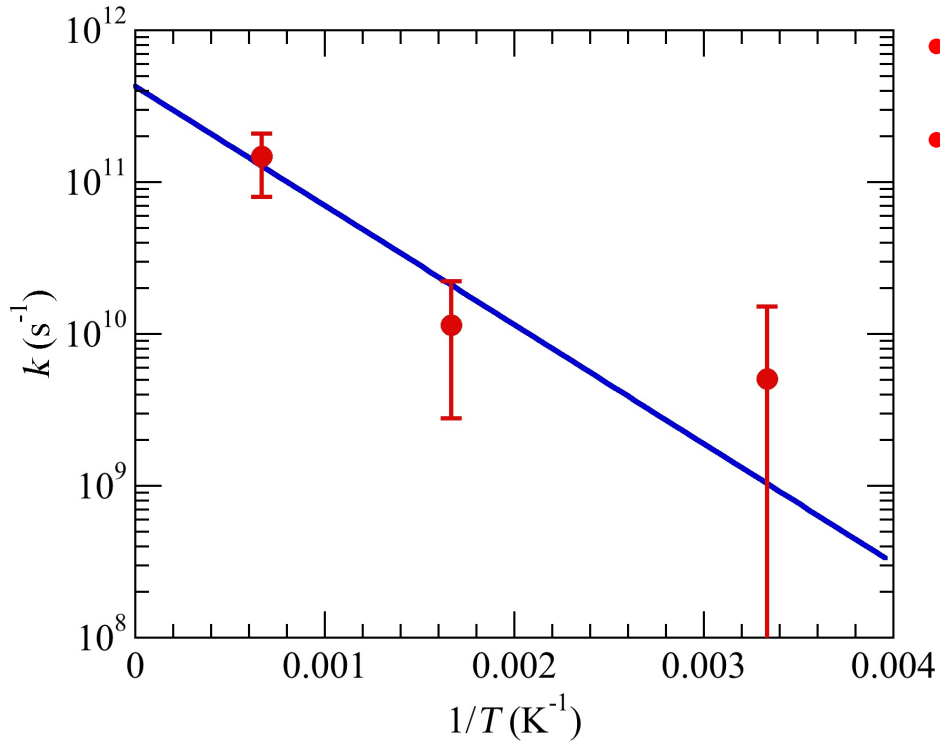
K. Shimamura *et al.*,  
*Nano Lett.* **14**, 4090 ('14)



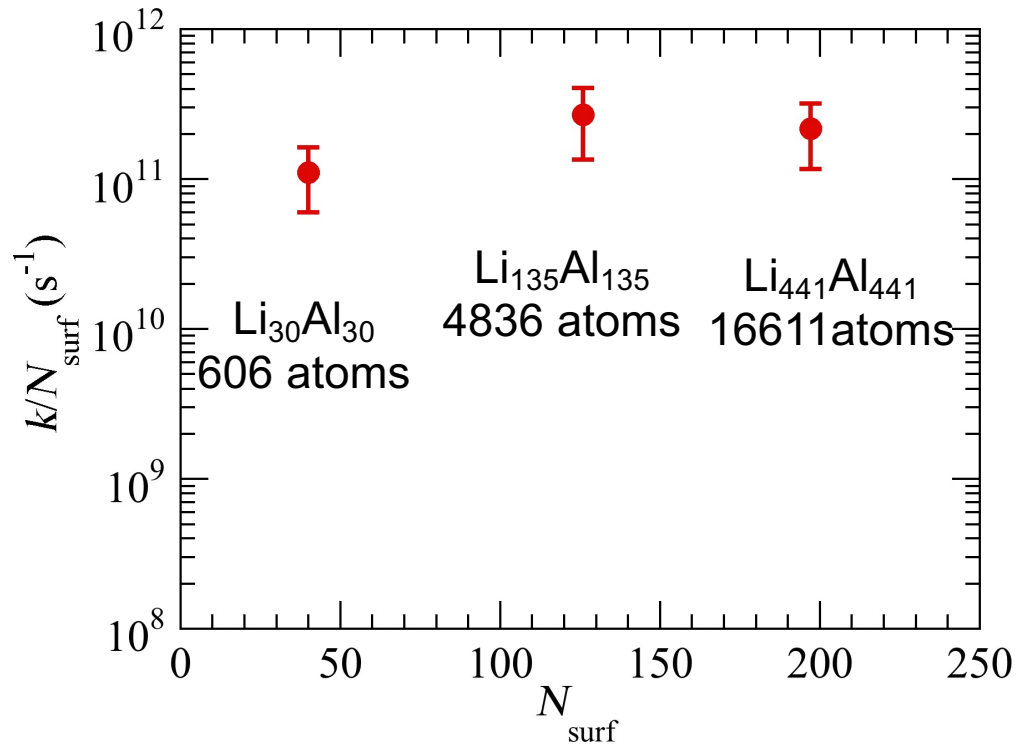
21,140 time steps (129,208 self-consistent-field iterations)

# Rapid & Scalable H<sub>2</sub> Production

- Orders-of-magnitude faster H<sub>2</sub> production from water than with pure Al



- Activation barrier = 0.068 eV
- Reaction rate =  $1.04 \times 10^9$  (s<sup>-1</sup>) per LiAl pair at 300 K

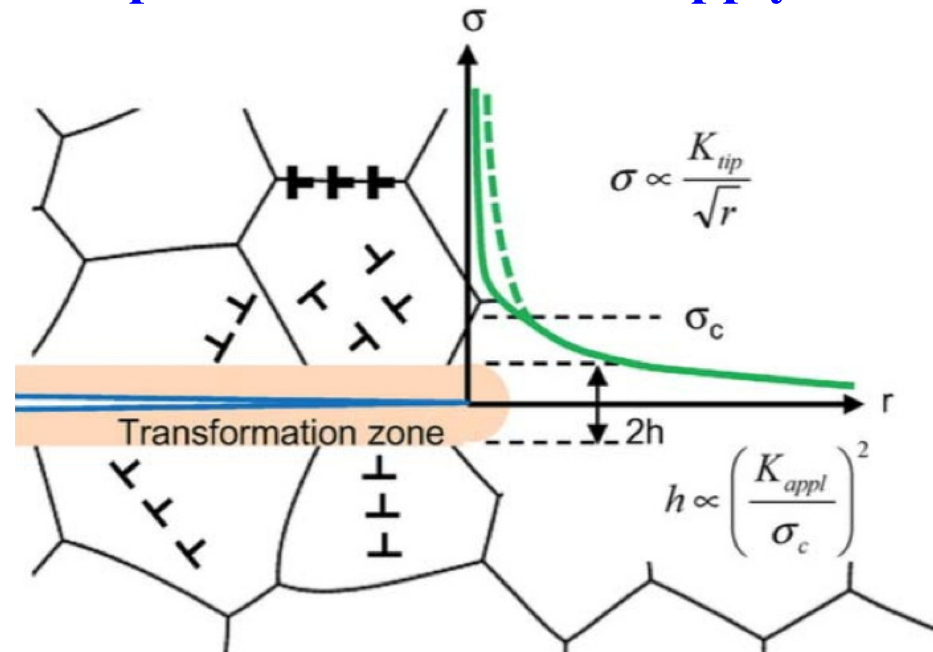
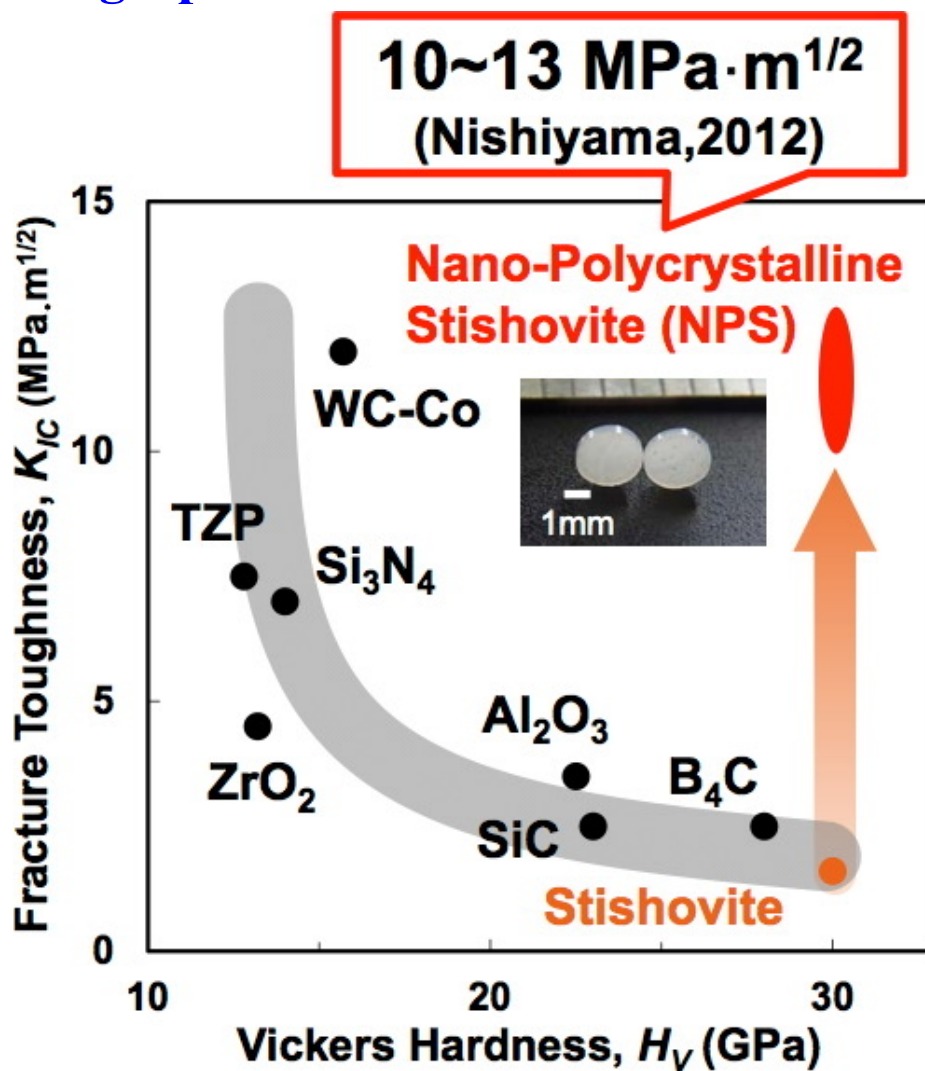


- Reaction rate does not decrease for larger particles → industrial scalability

K. Shimamura *et al.*, *Nano Lett.* **14**, 4090 ('14); K. Nomura *et al.*, *IEEE/ACM SC14* ('14)

# Crack Self-Healing Stishovite

- Superhard, ultratough nano-polycrystalline stishovite (NPS) synthesized  
N. Nishiyama *et al.*, *Scripta Mater.* **67**, 955 ('12); *Sci. Rep.* **4**, 6588 ('14)
- Made of Earth-abundant silica glass, NPS provides sustainable supply of high-performance ceramics

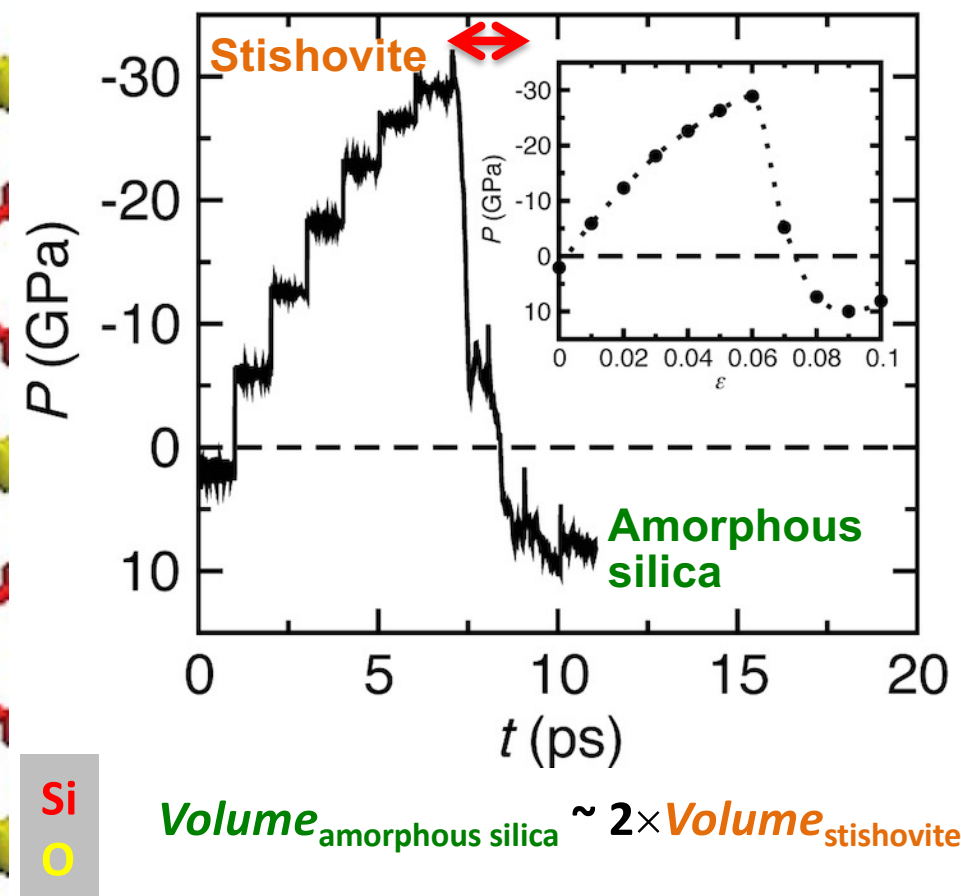
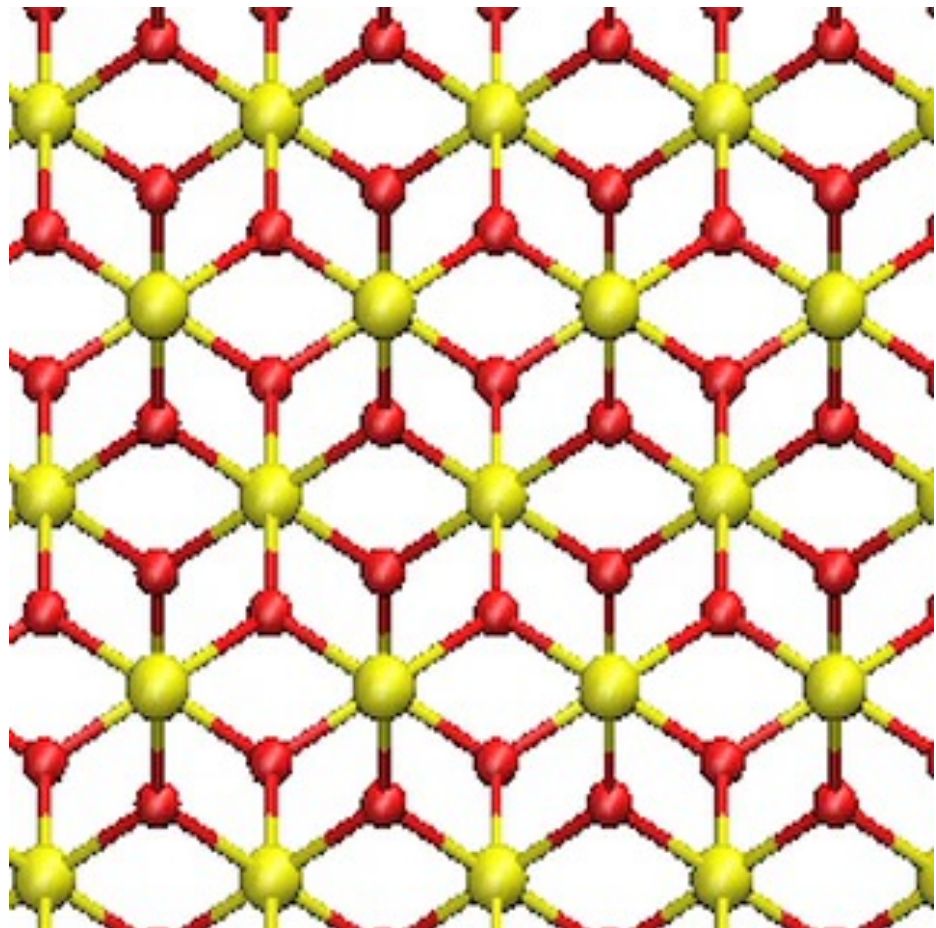


K. Yoshida *et al.*, *Sci. Rep.* **5**, 10993 ('15);  
*Acta Mater.* **124**, 316 ('17)

- Toughening mechanism hypothesized to be amorphization under tension
- To catch up with a fast moving crack, amorphization needs rapid, but no theoretical nor experimental evidence

# Rapid Tensile Amorphization

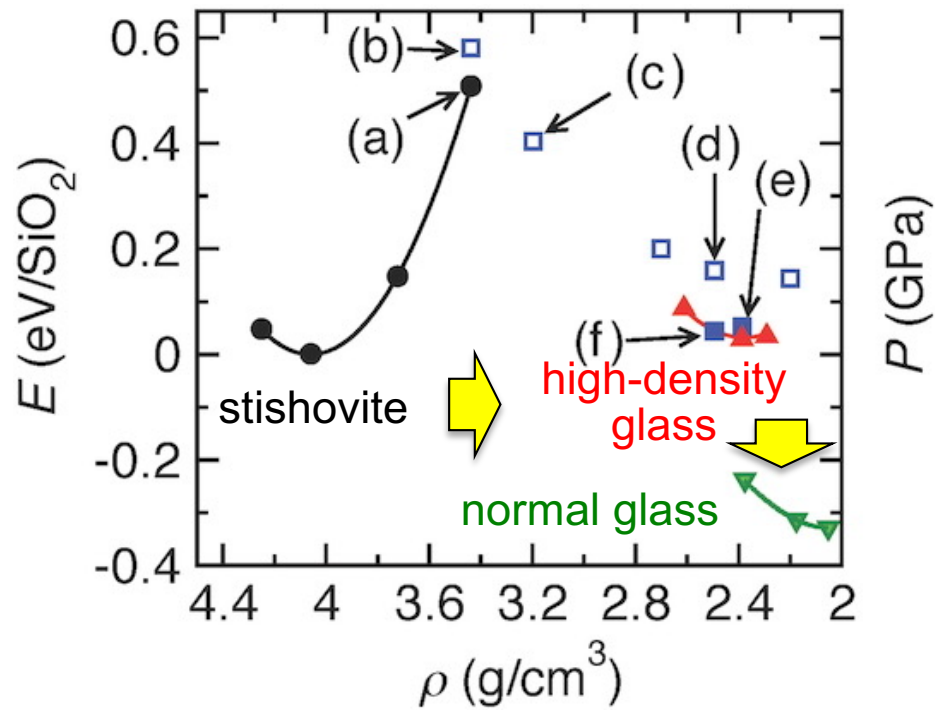
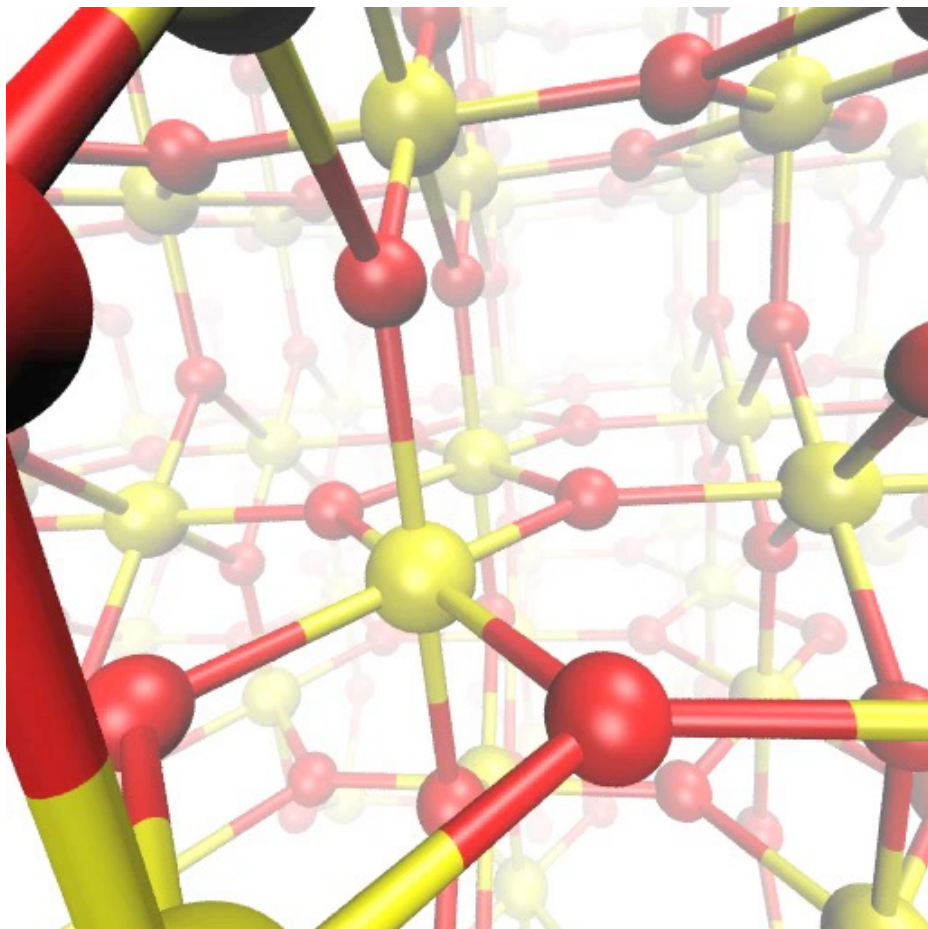
- QMD simulation reveals rapid amorphization of stishovite within picoseconds under tension  $\sim 30$  GPa



- The rapid & expansive amorphization can catch up with, screen & self-heal a fast moving crack

# Rapid Amorphization Mechanism

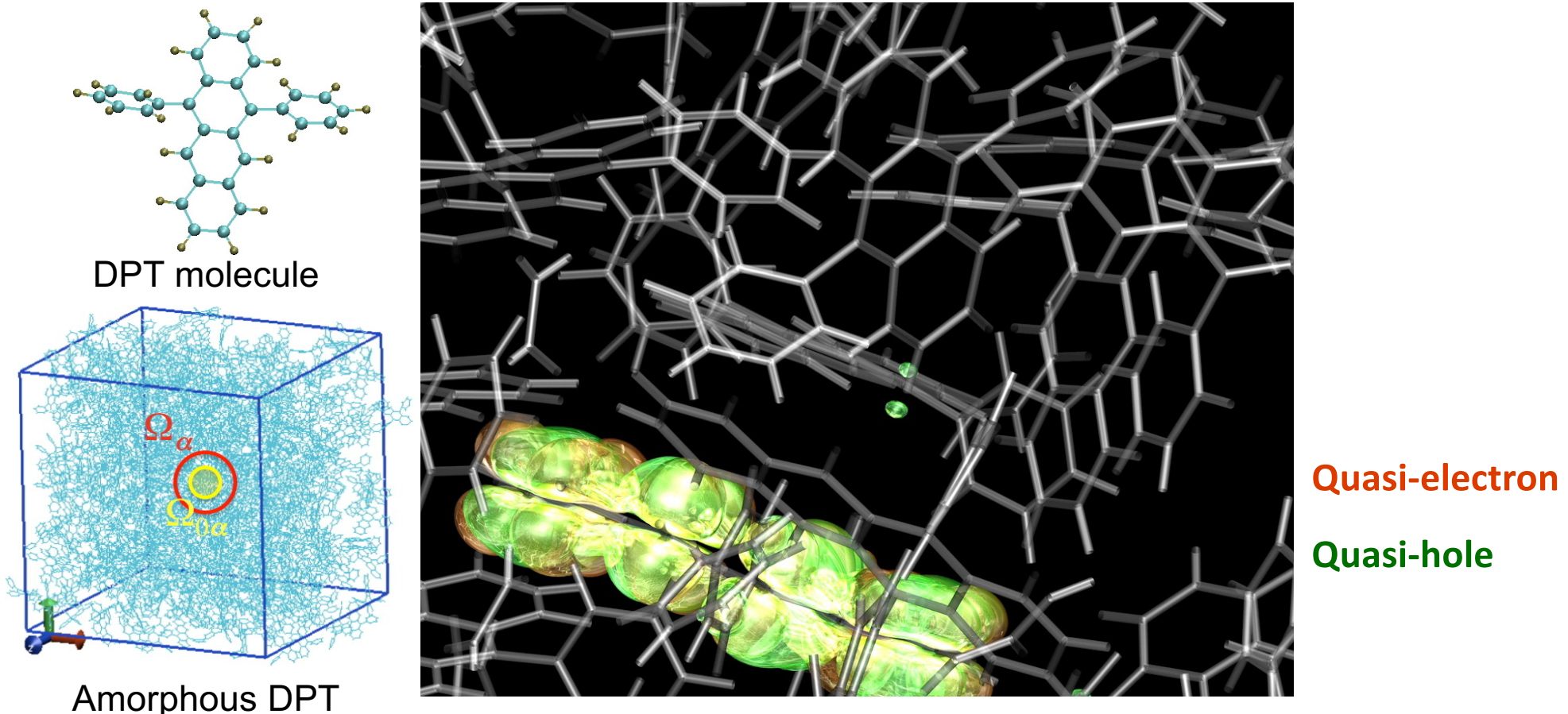
- Found a displacive amorphization mechanism that only involves short-distance collective motions of atoms, thereby facilitating the rapid transformation



- Two-step amorphization pathway from stishovite to glass involves an intermediate state akin to an experimentally suggested “high-density glass polymorph”

# Singlet Fission in Amorphous DPT

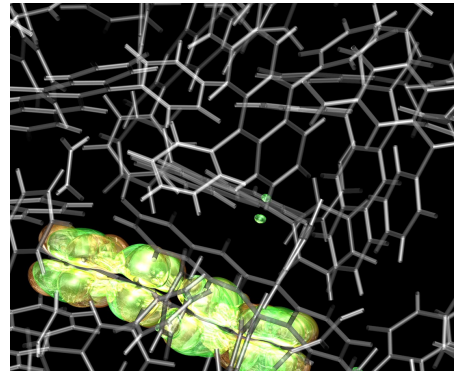
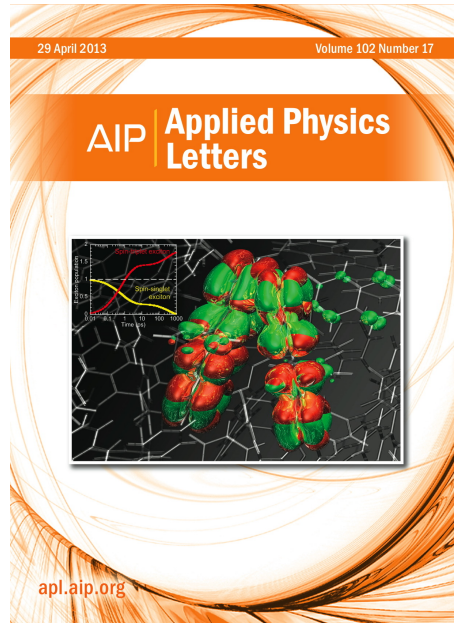
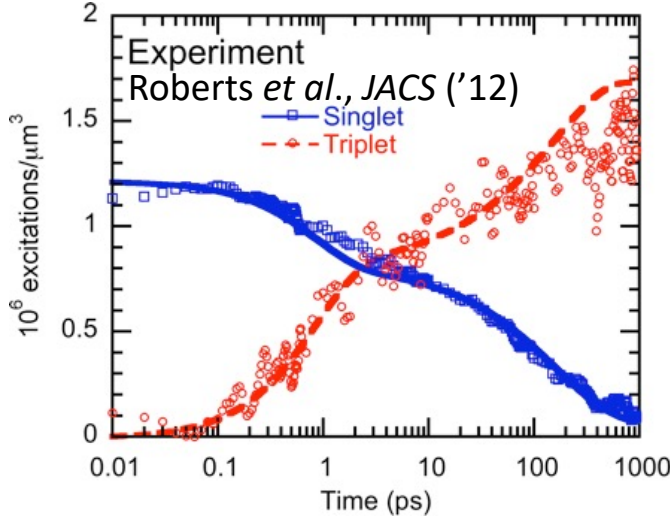
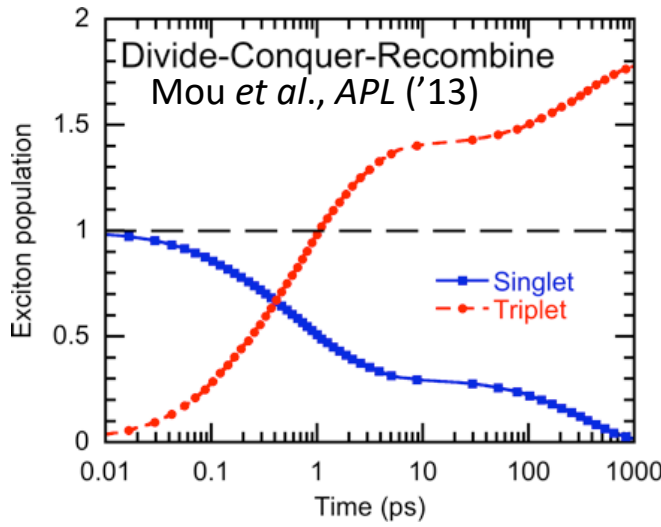
- Photo-current doubling by splitting a singlet exciton into 2 triplet excitons
- Singlet fission in mass-produced disordered organic solid → efficient low-cost solar cells
- Experimental breakthrough: SF found in amorphous diphenyl tetracene (DPT)



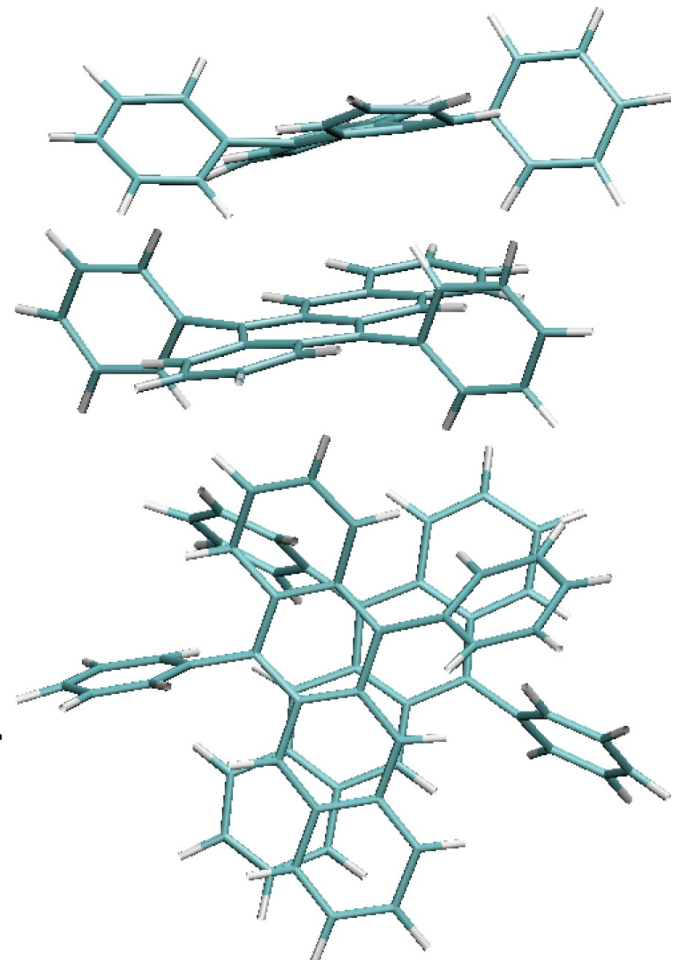
- Divide-conquer-recombine nonadiabatic QMD (phonon-assisted exciton dynamics) + time-dependent perturbation theory (singlet-fission rate) + kinetic Monte Carlo calculations of exciton population dynamics in 6,400-atom amorphous DPT

# Singlet-Fission Hot Spot

- Nonadiabatic quantum molecular dynamics simulations not only reproduced experimentally measured exciton population dynamics but also revealed unknown molecular geometry of singlet fission hot spots

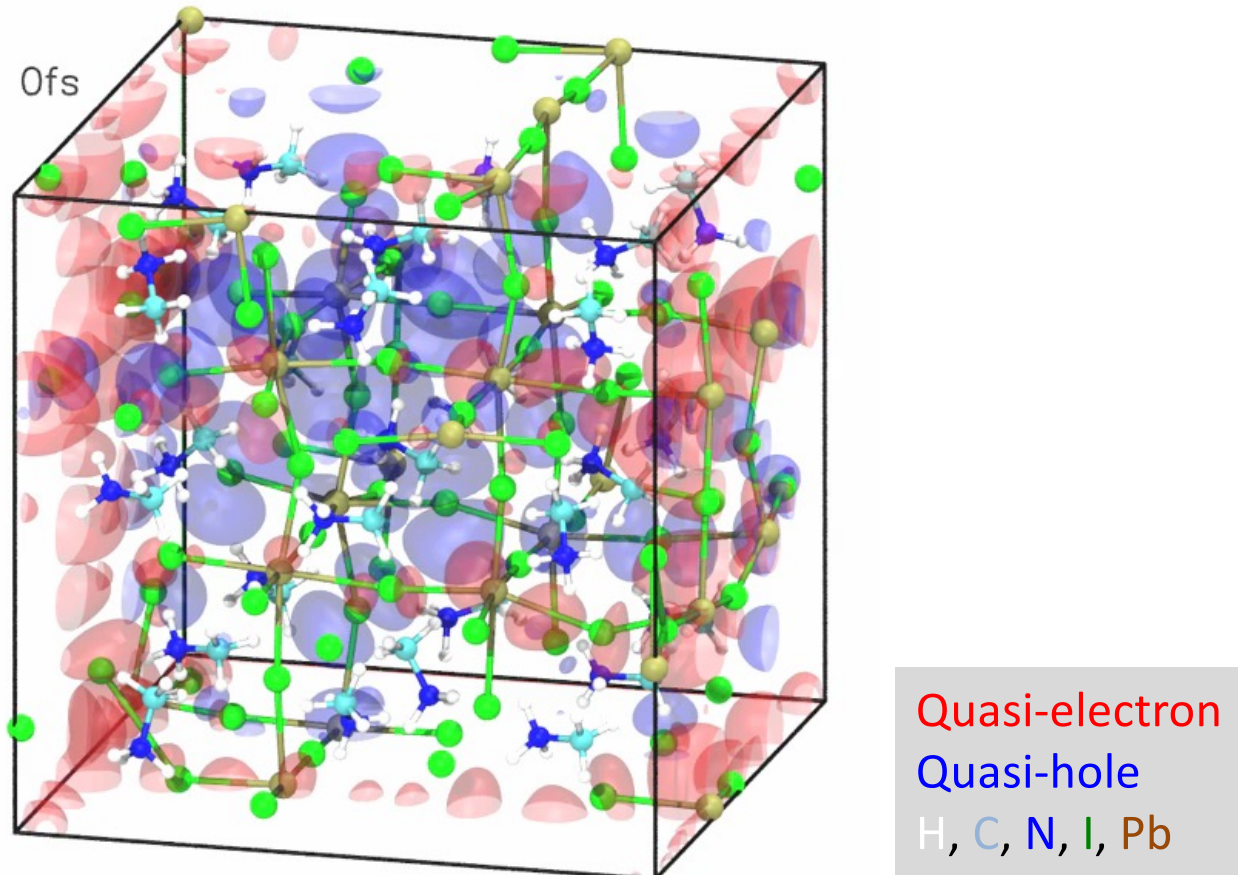


Side view  
Top view



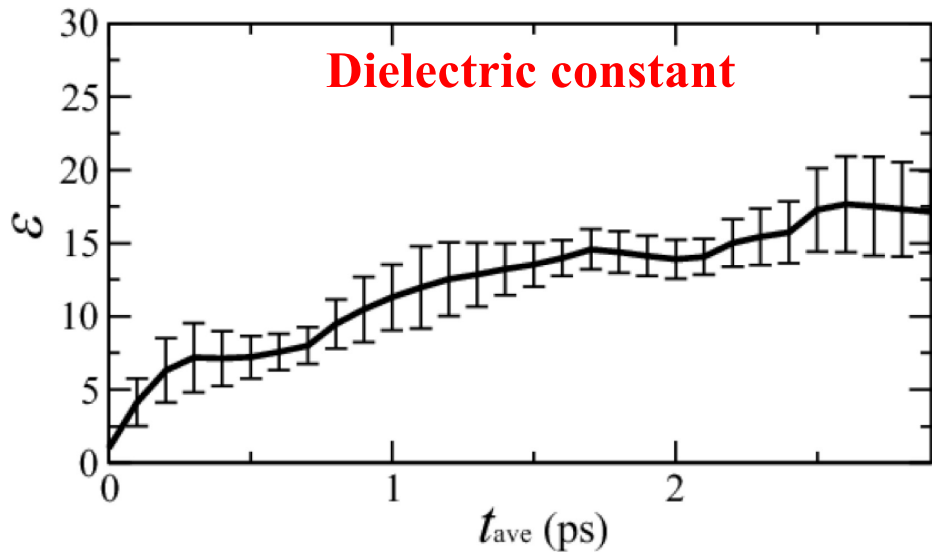
# Photoexcited Carriers in $\text{MAPbI}_3$

- Organometal halide perovskites (e.g. methylammonium lead iodide,  $\text{CH}_3\text{NH}_3\text{PbI}_3$  or  $\text{MAPbI}_3$ ) for solar cells with high power conversion efficiency > 20%  
[Stranks & Snaith, *Nat. Nanotechnol.* **10**, 391 ('15)]



- Nonadiabatic QMD simulation  
**Pb & I sublattices act as disjunct pathways for rapid & balanced transport of free electrons & holes — electron (63% Pb-6p) & hole (90% I-5p); diffusion coefficients  $D_e = (1.16 \pm 0.31) \times 10^{-2} \text{ cm}^2/\text{s}$  &  $D_h = (1.01 \pm 0.42) \times 10^{-2} \text{ cm}^2/\text{s}$**   
Expt:  $D_e = (1.7 \pm 1.1) \times 10^{-2} \text{ cm}^2/\text{s}$  &  $D_h = (1.1 \pm 0.7) \times 10^{-2} \text{ cm}^2/\text{s}$  [Stranks *et al.*, *Science* **342**, 341 ('13)]

# Screening Role of Methylammonium Sublattice

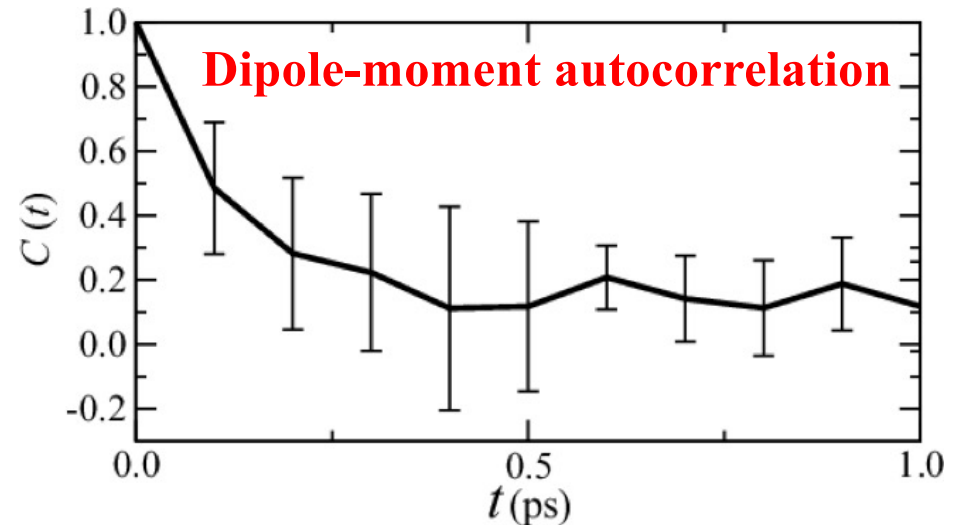


$$\varepsilon = 1 + \frac{4\pi}{3k_B TV} (\langle \mathbf{M}^2 \rangle - \langle \mathbf{M} \rangle^2)$$

time average  
dipole moment

cf.  $\varepsilon_{\text{expt}}(10^{12} \text{ Hz}) = 7-10$

Lin *et al.*, *Nat. Photonics* **9**, 106 ('15)



$$C(t) = \frac{\langle \mathbf{M}(t + t_0) \cdot \mathbf{M}(t_0) \rangle}{\langle \mathbf{M}(t_0) \cdot \mathbf{M}(t_0) \rangle}$$

**Rapid response time  $\sim 1$  ps**

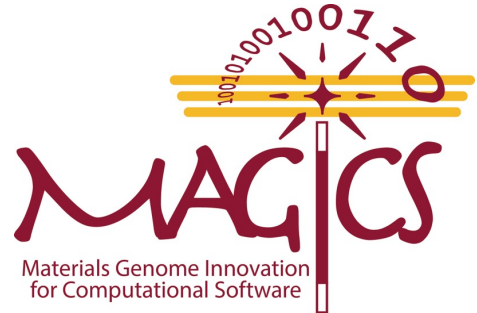
cf.  $\tau_{\text{expt}} = 2$  ps

Deschler *et al.*, *JPCL* **5**, 1421 ('15)

- Large dielectric constant of MA sublattice causes small exciton binding energy,  $0.012 \pm 0.009$  eV (experimental upper bound = 0.05 eV [D'Innocenzo *et al.*, *Nat. Commun.* **5**, 3586 ('14)])
- MA sublattice quickly screens out electrostatic electron-hole attraction to unbind an exciton & generate free carriers within 1 ps [cf. Zhu *et al.*, *Science* **353**, 1409 ('16)]

Hakamata *et al.*, *Sci. Rep.* **5**, 19599 ('16)

# MAterials Genome Innovation for Computational Software



U.S. DEPARTMENT OF  
**ENERGY**

Basic Energy Sciences

Office of  
Science

Priya Vashishta-PI, Malancha Gupta, Rajiv K. Kalia, Aiichiro Nakano,  
Oleg Prezhdo *University of Southern California*

Uwe Bergmann and David Fritz *Linac Coherent Light Source, SLAC*

William A. Goddard, III *California Institute of Technology*

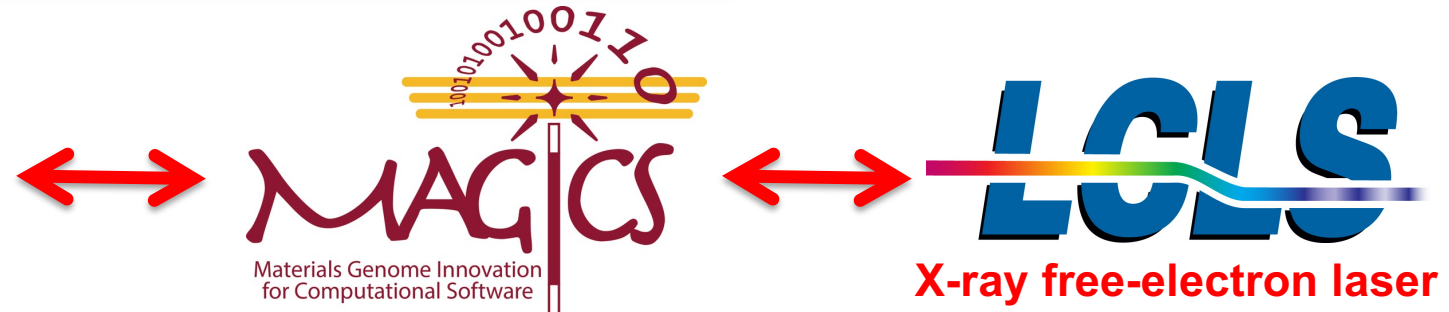
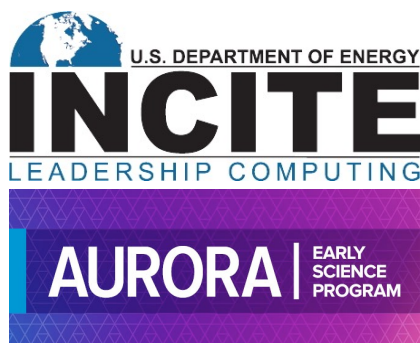
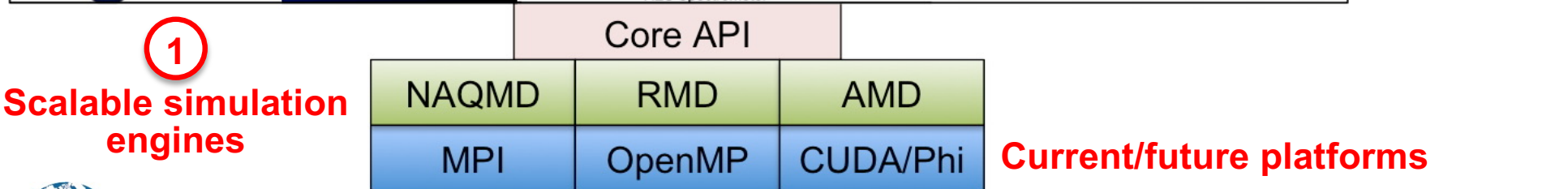
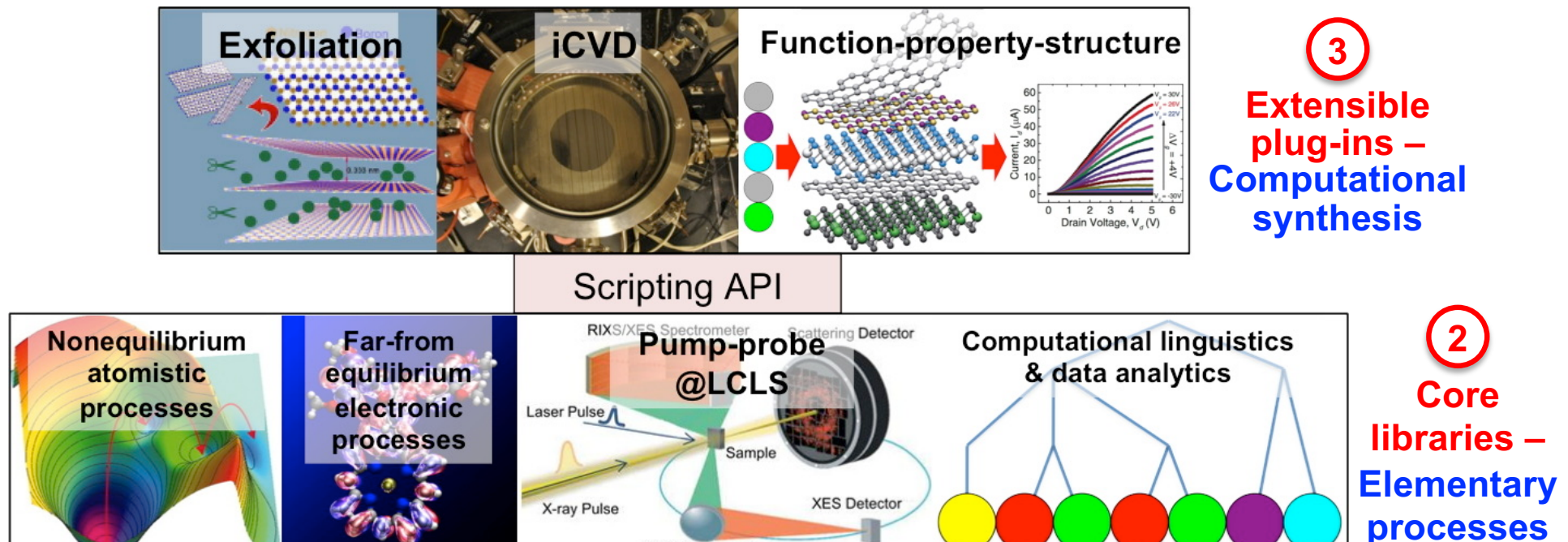
Kristin A. Persson *Lawrence Berkeley National Laboratory*

David J. Singh *University of Missouri*

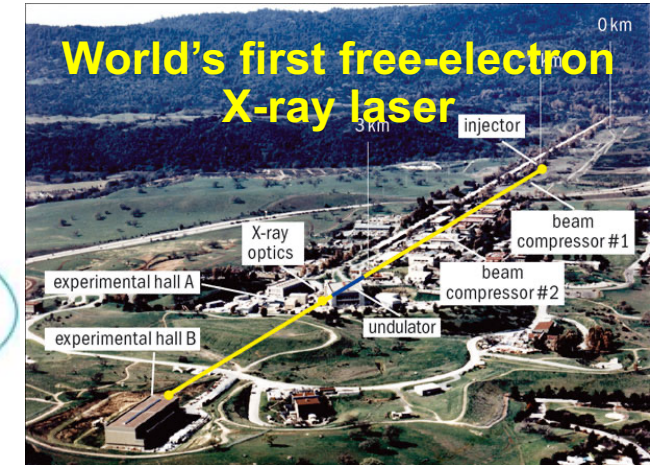
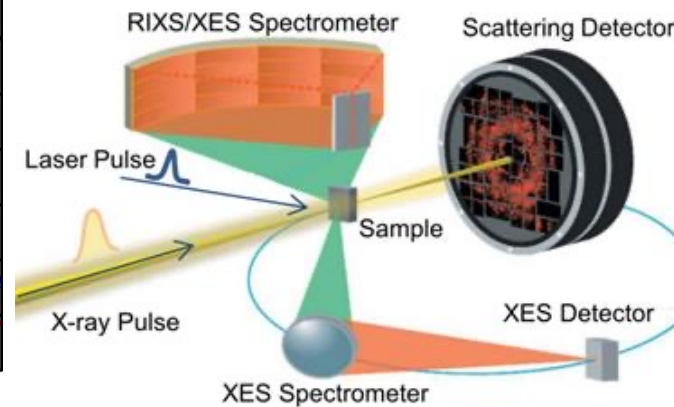
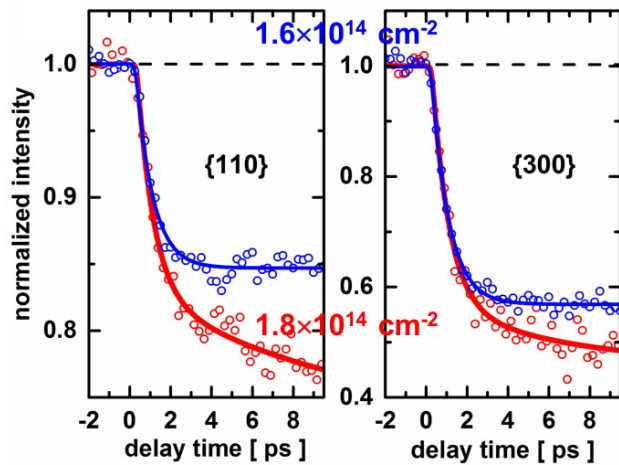
Pulickel M. Ajayan *Rice University*



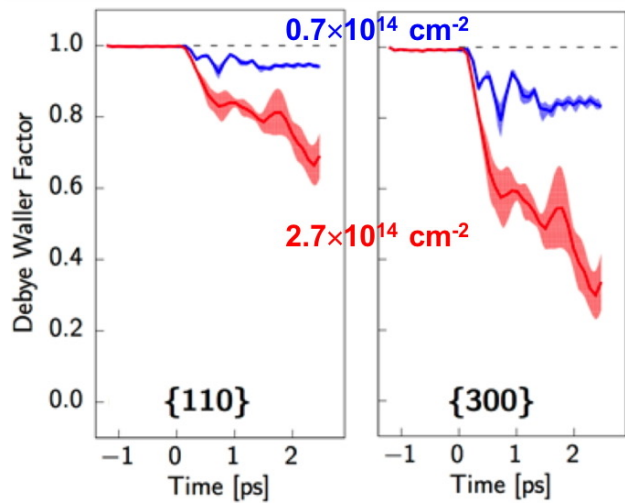
# Computational Synthesis of Functional Layered Materials: MAGICS Software Stack



# INCITE/AURORA-MAGICS-LCLS Synergy

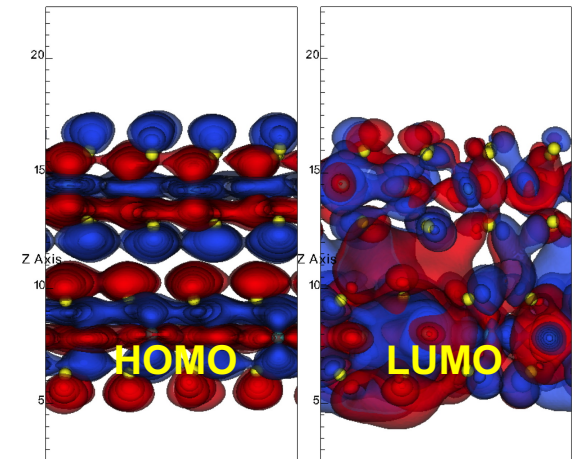
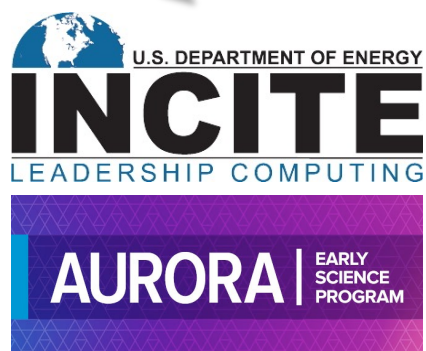


DOE INCITE & Aurora ESP  
Awards



Linac Coherent Light Source

LCLS

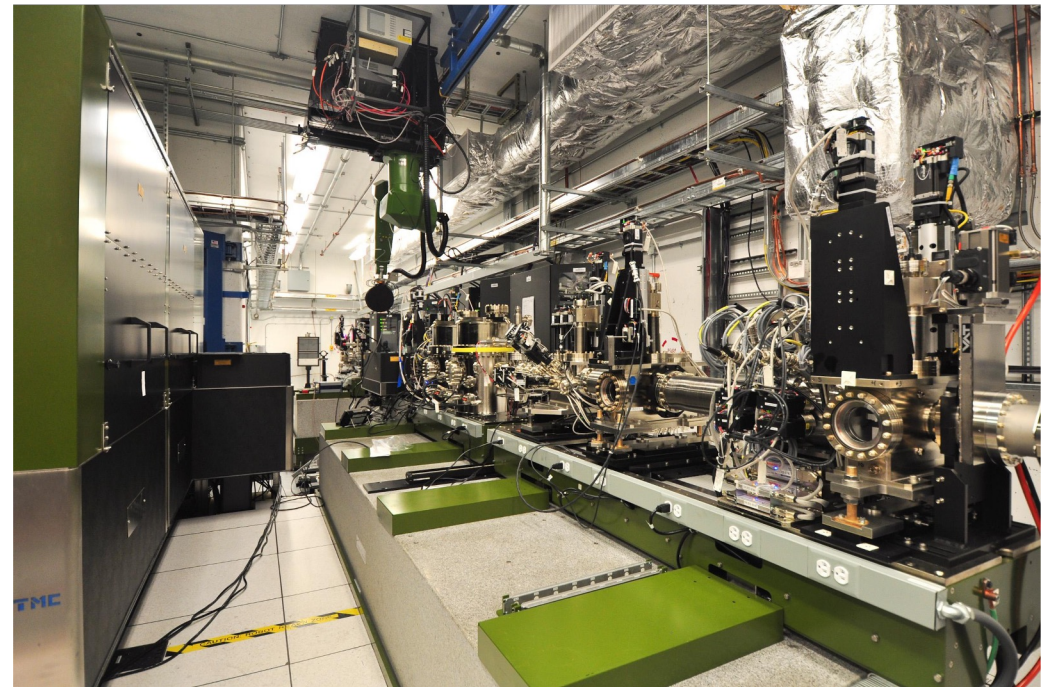
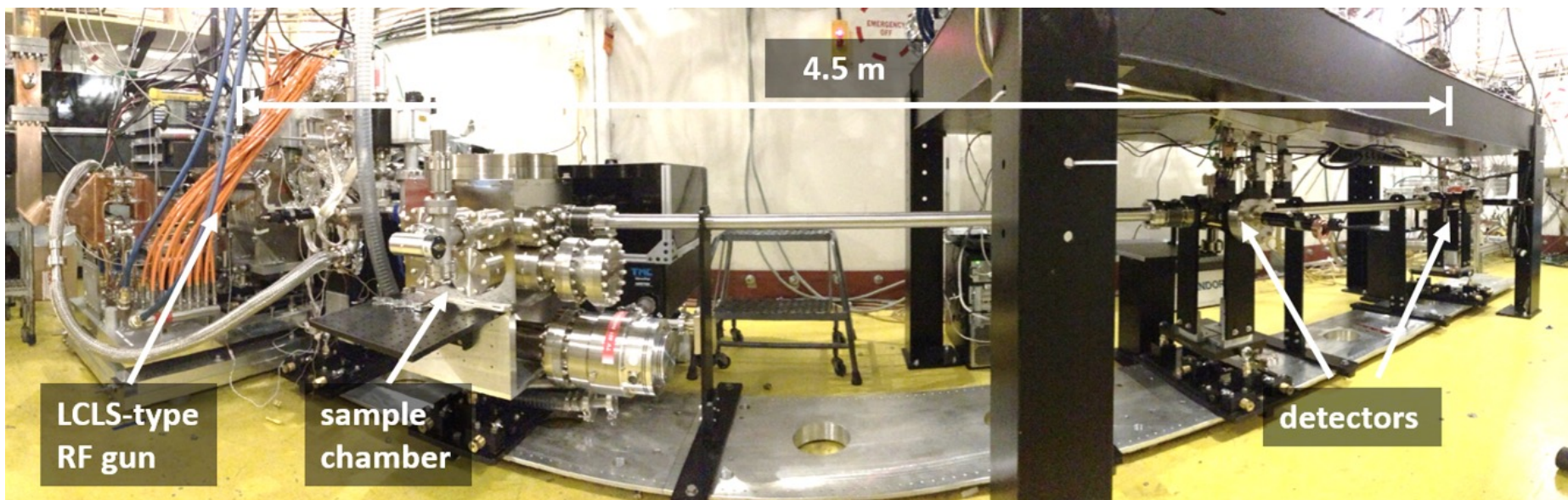


# ULTRAFAST PUMP-PROBE EXPERIMENTS

X-ray pump-probe (XPP)  
instrument: 4-25 KeV

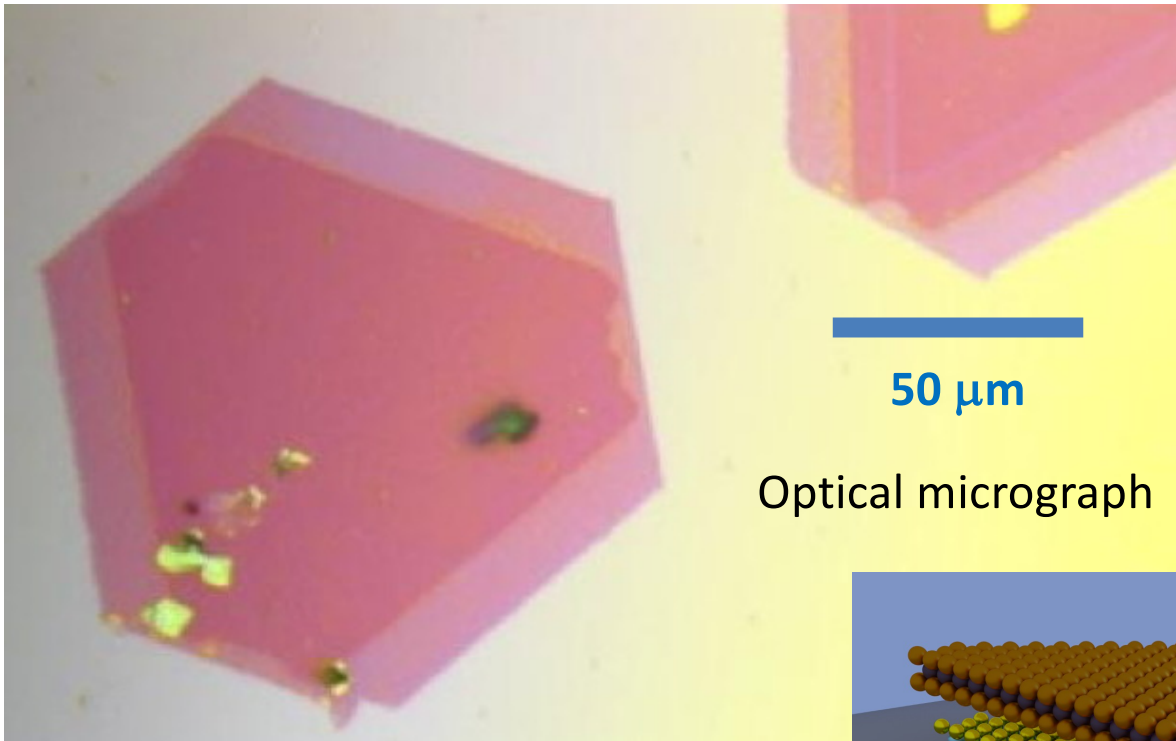


Ultrafast electron diffraction  
(UED) instrument: 3-5 MeV

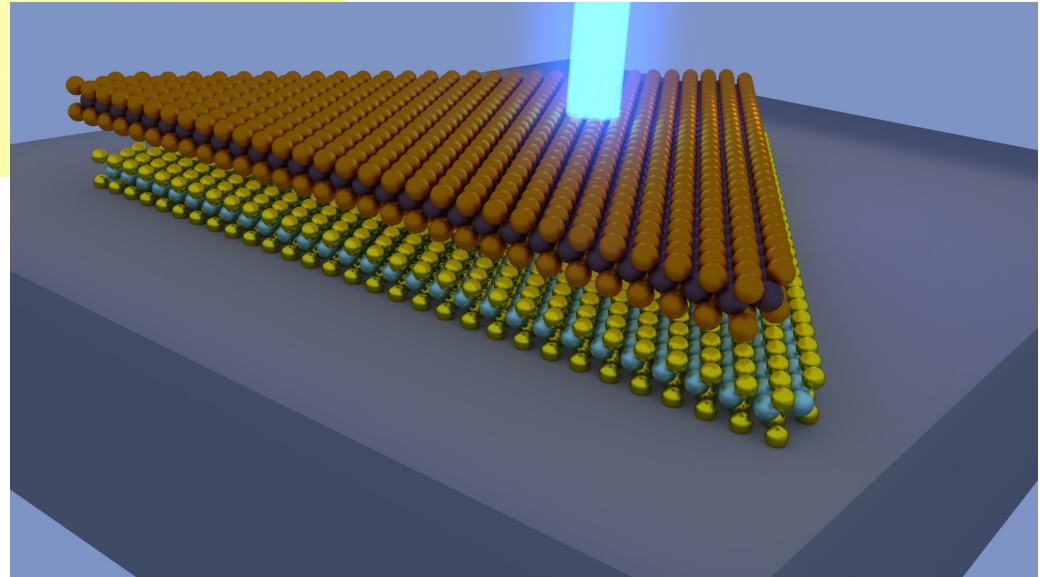


# 2D Transition Metal Dichalcogenide (TMDC)

- Mono- and bi-layer MoSe<sub>2</sub> synthesized by the Rice group (P. Ajayan)



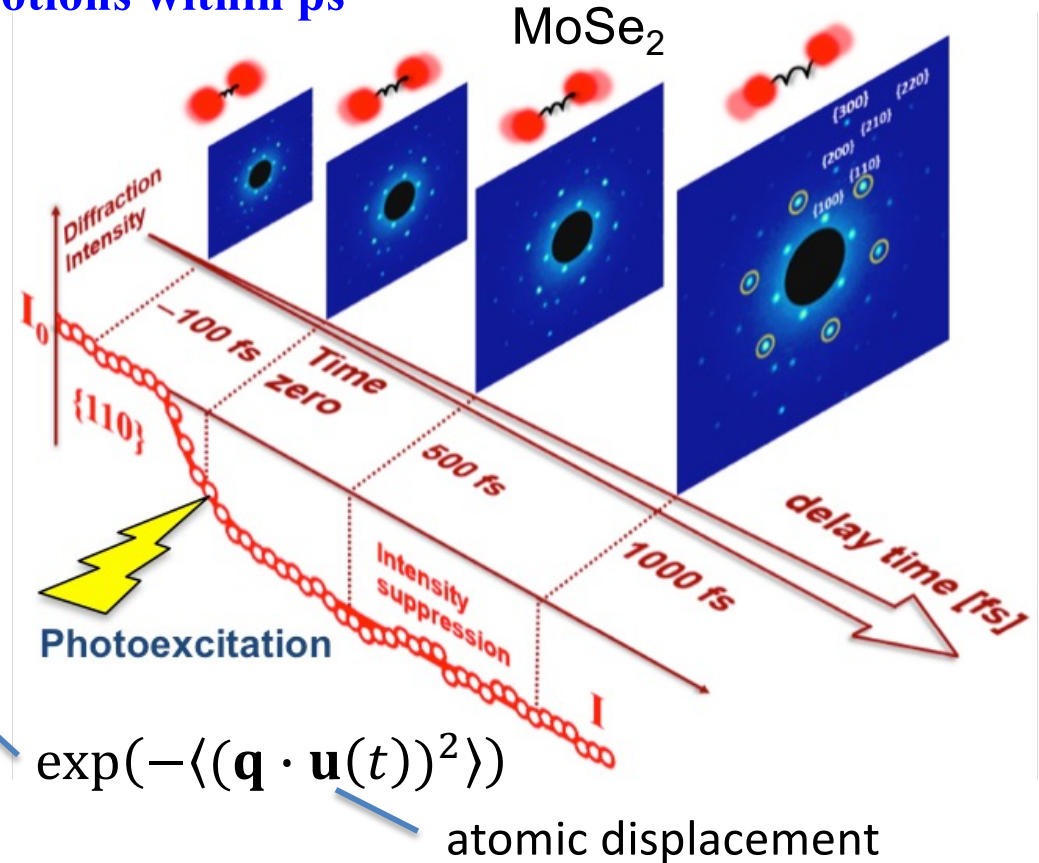
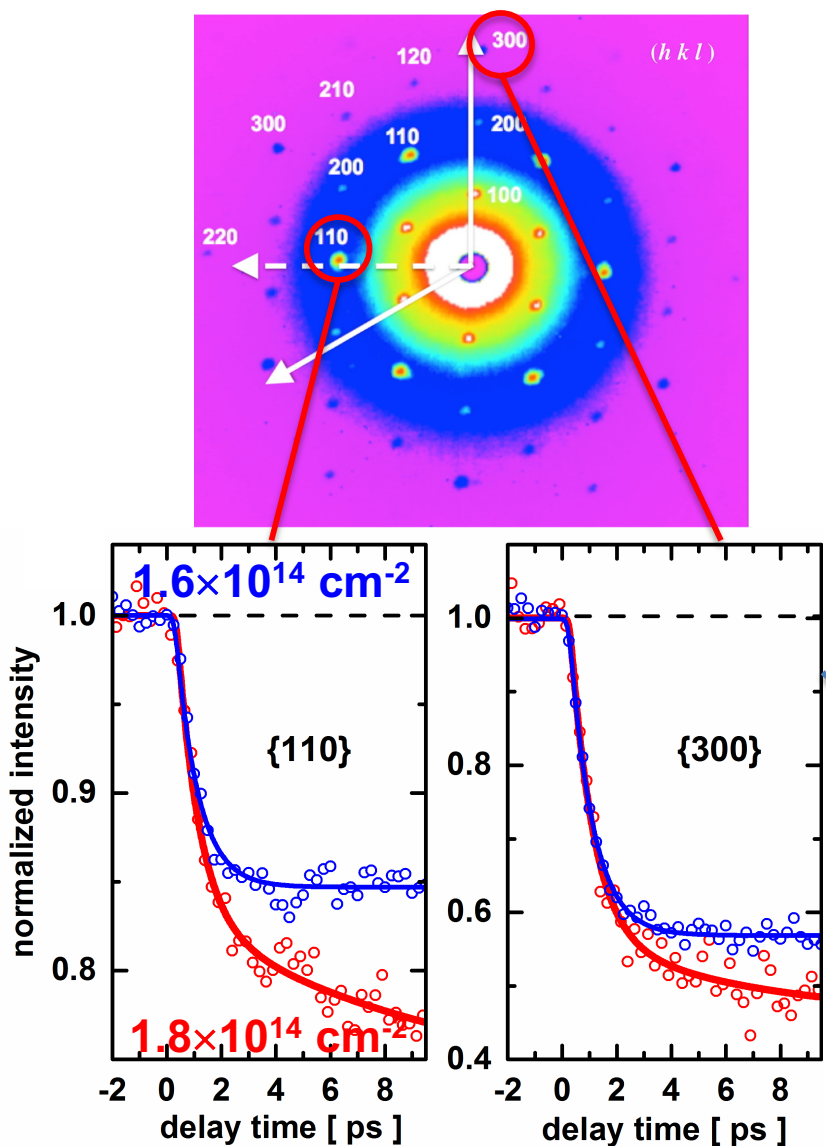
Optical micrograph



- **Question:** What is the nature of optically induced lattice dynamics for photo-patterning (e.g., semiconducting 2H to metallic 1T' phases) of TMDC?

# Ultrafast Coupled Electron-Lattice Dynamics

- Ultrafast electron diffraction experiment shows nearly perfect energy conversion from electronic excitation to lattice motions within ps

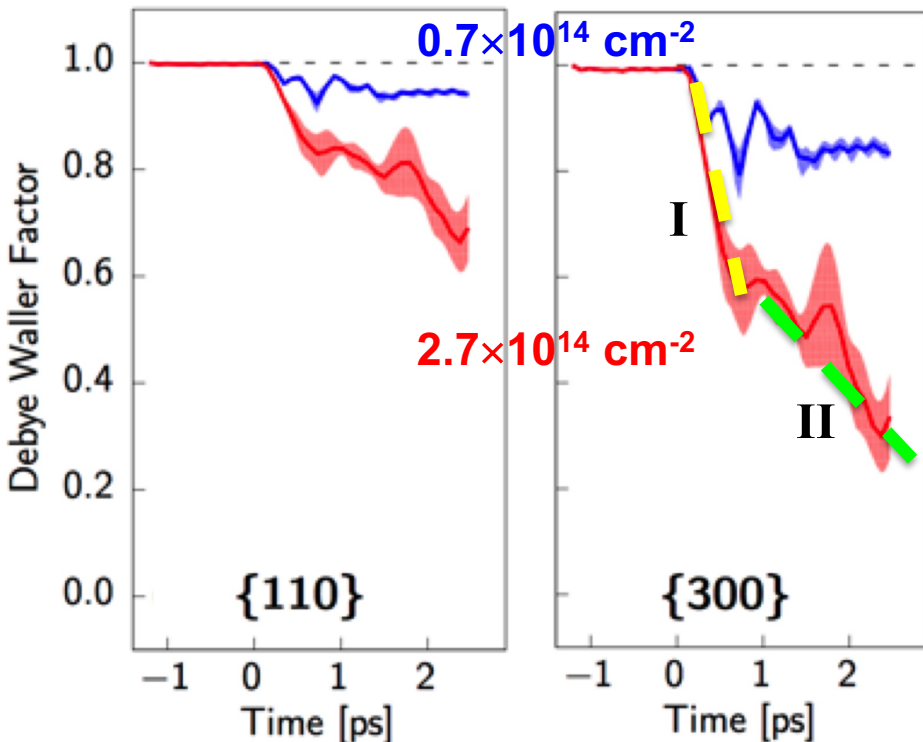


- Dynamics of Debye-Waller factor reveals rapid disordering for both {300} & {110} peaks
- Transition from mono- to bi-exponential decay at higher electron-hole density

M.F. Lin *et al.*, *Nature Commun.* **8**, 1745 ('17)

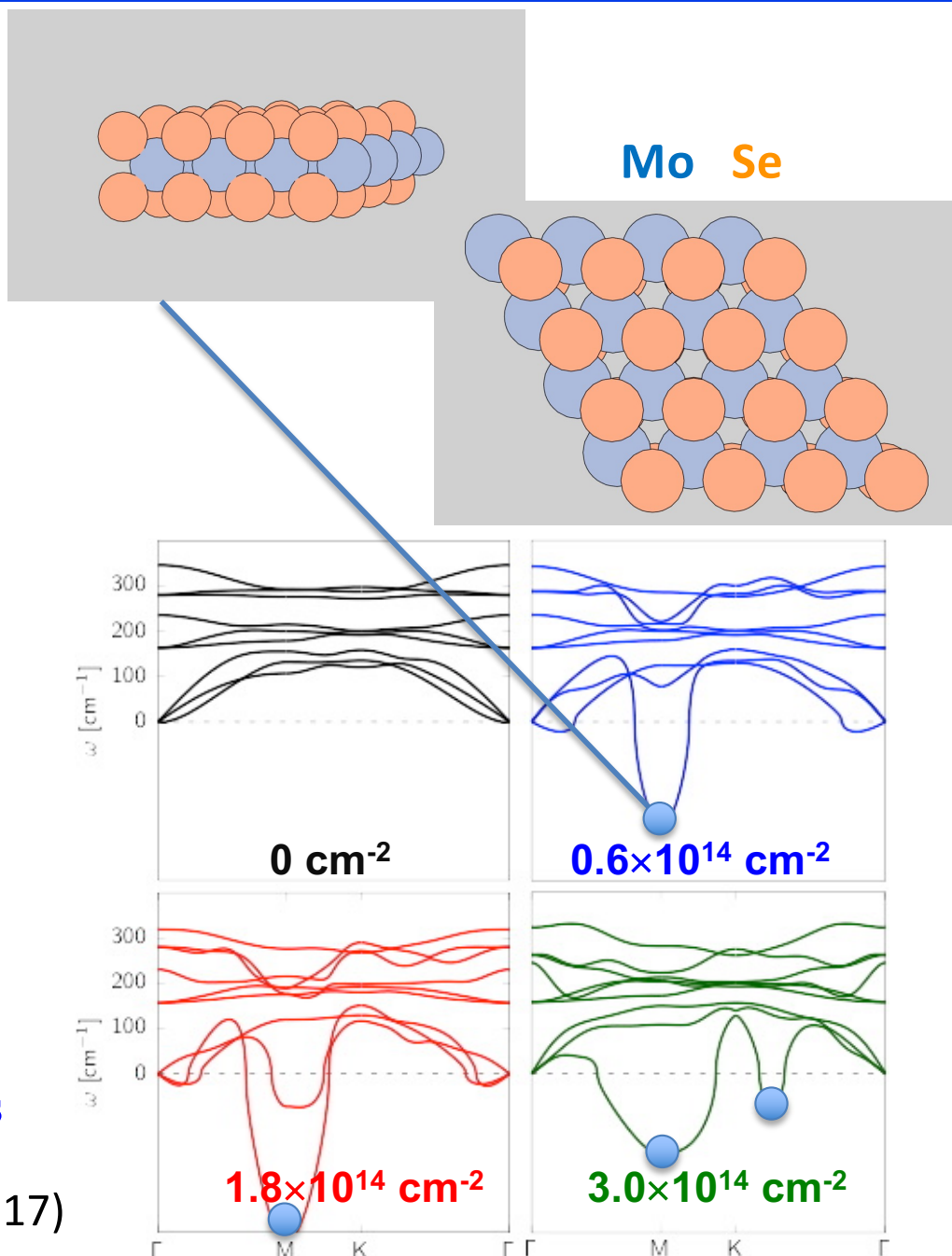
# Strong Electron-Lattice Coupling

- NAQMD simulations reproduce (1) rapid photo-induced lattice dynamics & (2) mono- to bi-exponential transition at higher electron-hole density



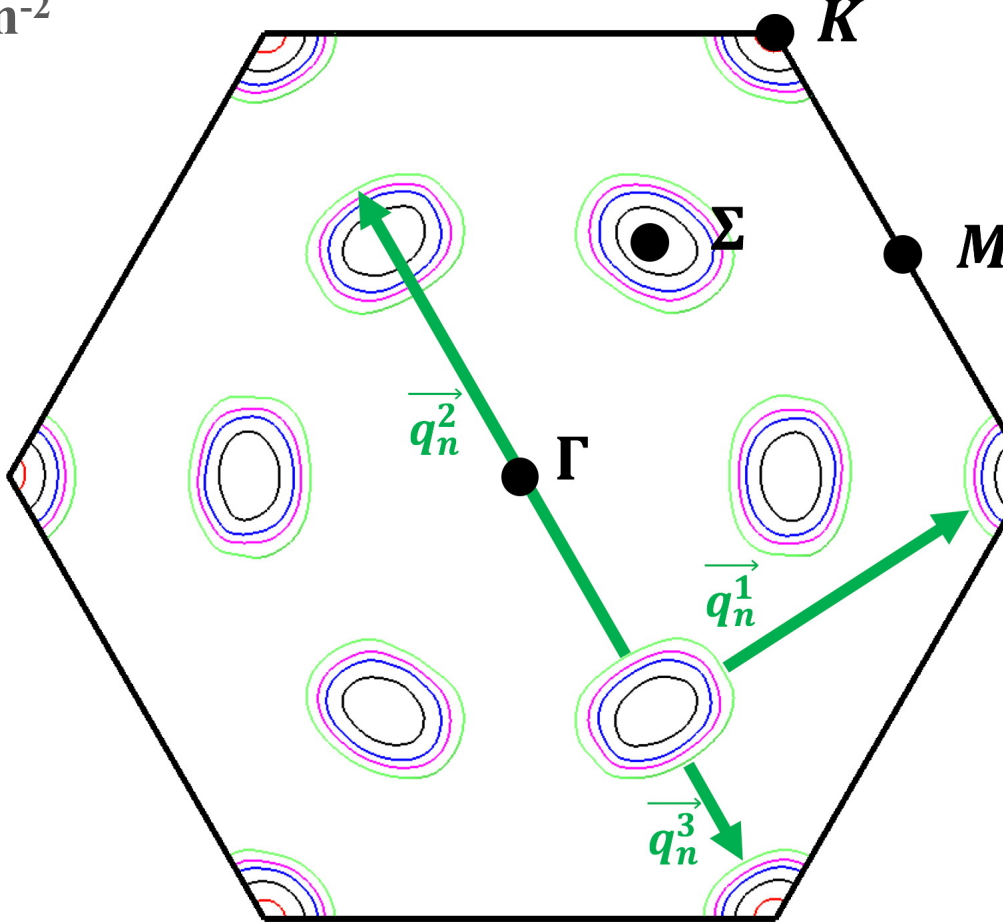
- Rapid lattice dynamics is explained by the softening of M-point ( $\frac{1}{2} 0 0$ ) phonon
- Bi-exponential transition is explained by the softening of additional phonon modes at higher electron-hole densities

M.F. Lin *et al.*, *Nature Commun.* **8**, 1745 ('17)



# Electronic Origin of Phonon Softening

- Electronic Fermi surface for the electron-hole density  $n(\text{e-h})$  ranging from 0.2 to  $2 \times 10^{14} \text{ cm}^{-2}$

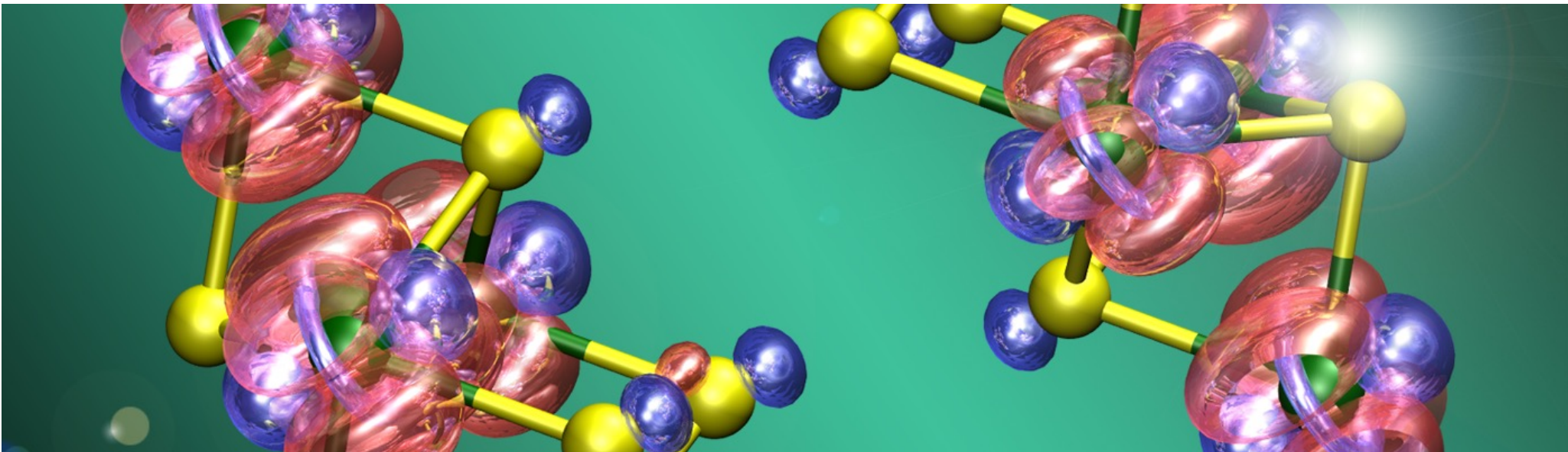


$$n(\text{e-h}) = 0.22, 1, 2, 3, 4 \times 10^{14} \text{ cm}^{-2}$$

- While the Fermi surface is localized at  $K$ -points at minimal excitation (red), it occupies  $\Sigma$ -pockets at larger  $n(\text{e-h})$  (black & blue), enabling electron scattering by emitting  $\vec{q}_n^1$  ( $M$ ),  $\vec{q}_n^2$  ( $\Sigma$ ) and  $\vec{q}_n^3$  ( $K$ ) phonons

# Simulation-Experiment Synergy

---

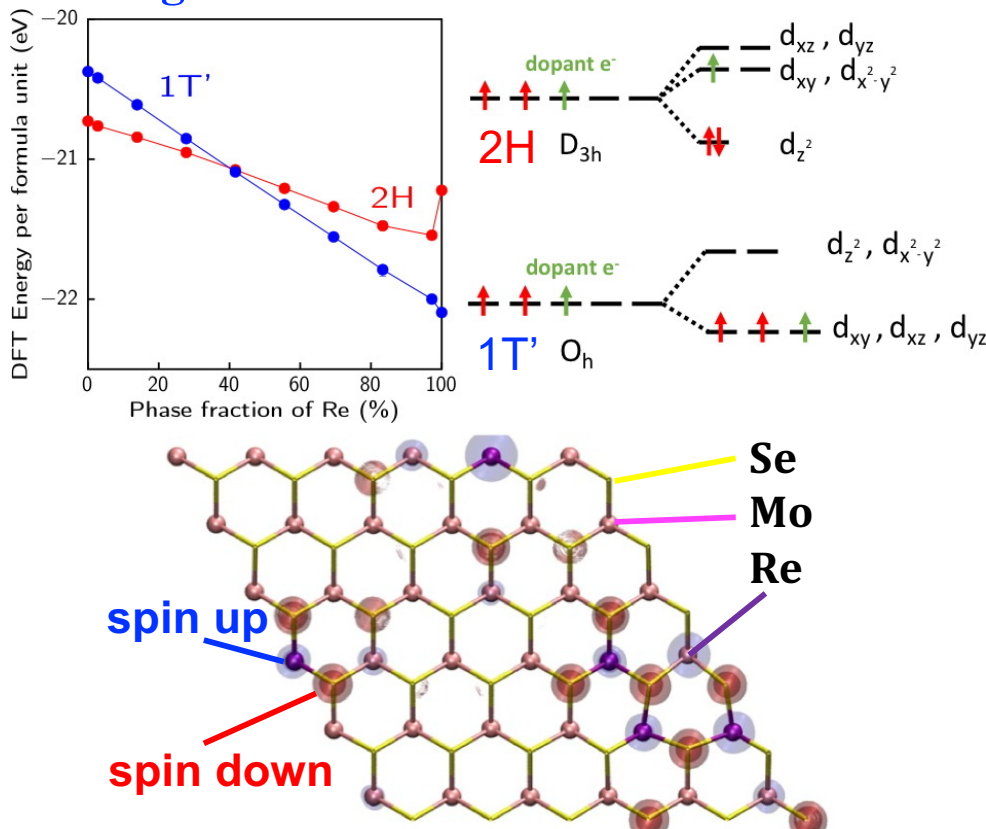


- In the ultrafast ‘electron camera,’ laser light hitting a material is almost completely converted into nuclear vibrations — key to switching material properties on & off at will for future electronics applications
- High-end quantum simulations reproduce the ultrafast energy conversion at exactly the same space & time scales, & explain it as a consequence of photo-induced phonon softening

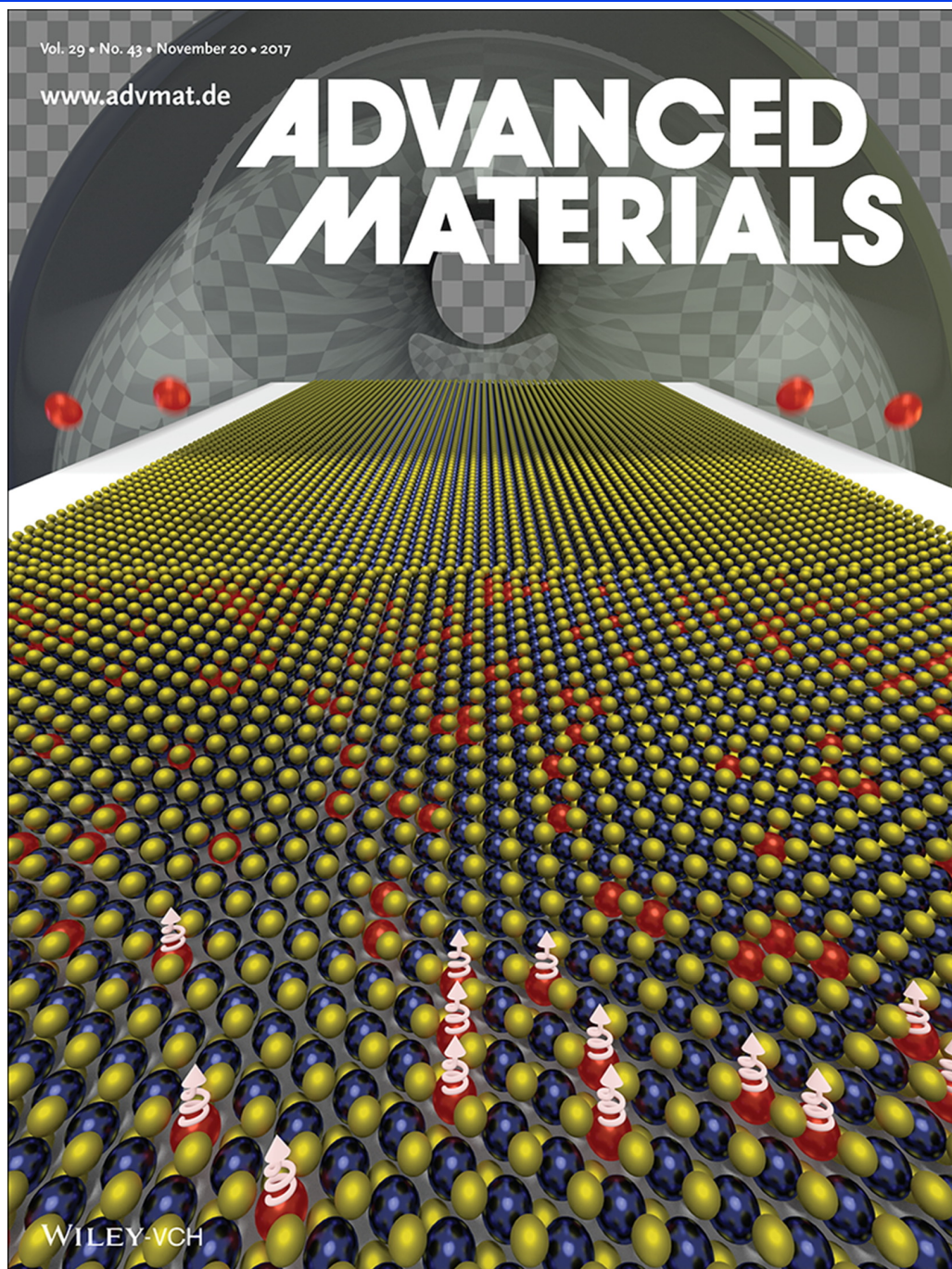
M.F. Lin *et al.*, *Nature Commun.* **8**, 1745 ('17)

# Semiconductor-to-Metal Transition via Doping

- Experiment at Rice shows 2H-to-1T' phase transformation by alloying MoSe<sub>2</sub> with Re
- QMD simulations at USC elucidate its electronic origin
- Simulation & experiment show novel magnetism centered at Re atoms



V. Kochat *et al.*, *Adv. Mater.* **29**, 1703754 ('17)



# Conclusion

1. Large spatiotemporal-scale quantum molecular dynamics simulations enabled by divide-conquer-recombine
2. Broad materials & energy applications

